NANO · MICRO small
www.small-journal.com

A Review on Recent Advances for Boosting Initial Coulombic Efficiency of Silicon Anodic Lithium Ion batteries

Lin Sun, Yanxiu Liu, Jun Wu, Rong Shao, Ruiyu Jiang, Zuoxiu Tie, and Zhong Jin**

Rechargeable silicon anode lithium ion batteries (SLIBs) have attracted tremendous attention because of their merits, including a high theoretical capacity, low working potential, and abundant natural sources. The past decade has witnessed significant developments in terms of extending the lifespan and maintaining high capacities of SLIBs. However, the detrimental issue of low initial Coulombic efficiency (ICE) toward SLIBs is causing more and more attention in recent years because ICE value is a core index in full battery design that profoundly determines the utilization of active materials and the weight of an assembled battery. Herein, a comprehensive review is presented of recent advances in solutions for improving ICE of SLIBs. From design perspectives, the strategies for boosting ICE of silicon anodes are systematically categorized into several aspects covering structure regulation, prelithiation, interfacial design, binder design, and electrolyte additives. The merits and challenges of various approaches are highlighted and discussed in detail, which provides valuable insights into the rational design and development of state-of-the-art techniques to deal with the deteriorative issue of low ICE of SLIBs. Furthermore, conclusions and future promising research prospects for lifting ICE of SLIBs are proposed at the end of the review.

1. Introduction

Rechargeable lithium-ion batteries (LIBs) have received much attention and have been widely used as power supplies for portable electronics and electric vehicles since their first commercialization in 1991.[1] In 2019, the Nobel prize was awarded to John B Goodenough, M. Stanley Whittingham and Akira Yoshino, which fulfilled a long-cherished wish for researchers dedicated to studies of batteries. Although LIBs represent a sophisticated technique and have undergone many developments in recent decades, the current LIBs cannot meet the increasing demand for high energy and power density owing to the low specific capacity of graphite anodes.[2] Thus, it is essential and urgent to develop novel electrode materials with high theoretical capacities, that can effectively broaden the operating potential window of LIBs. With regard to anodic materials, silicon (Si) has attracted widespread concerns in the past decade as one of the most promising anodes because of its ultrahigh theoretical capacity (3579 mA h g^{-1}), low operating voltage (0.1–0.5 V vs Li/Li^+), and natural abundance (Si is the second most abundant element in the Earth's crust).[3]

Undoubtedly, Si anode lithium ion batteries (SLIBs) provide an exciting blueprint for supplying energy more efficiently. However, it should be noted that there are still some critical issues that need to be addressed, mainly including the large volume changes during lithiation/delithiation process, inherent poor electric conductivity of semiconducting Si, formation of unstable solid electrolyte interface (SEI) films, and low initial Coulombic efficiency (ICE).[4] To date, tremendous efforts have been devoted to design delicate structures of Si composites or to synthesize Si with controllable sizes and/or morphologies to accommodate the volume expansion resulting from aforementioned issues.[5]

On the other hand, the problem of low ICE for SLIBs is aroused increasing attention in recent years because the ICE value is a core index in full battery design that profoundly determines the utilization rate of active materials and the total weight of an assembled battery.[6] In current research stage, most of research works stem from SLIBs are in the laboratory. Although the formation of SEI films and the side reactions that occurred in the first lithiation process will result in severe problems relating to the cycle stability and the lifetime. However, in experimental studies, the counter electrode is usually constructed with metallic Li plates, which are considered as inexhaustible. Meanwhile, the low loading amount of Si slurry on the current collector will not weaken the cycle stability and lifespan of the half battery significantly. As a matter of fact, the limited supply of Li^+ in a full battery is mainly stem from the lithium-containing cathode. Any loss

L. Sun, Y. Liu, J. Wu, R. Shao, R. Jiang
School of Chemistry and Chemical Engineering
Yancheng Institute of Technology
Yancheng 224051, China
E-mail: sunlin@nju.edu.cn
L. Sun, Z. Tie, Z. Jin
MOE Key Laboratory of Mesoscopic Chemistry
MOE Key Laboratory of High Performance Polymer Materials and Technology
Jiangsu Key Laboratory of Advanced Organic Materials
School of Chemistry and Chemical Engineering
Nanjing University
Nanjing 210023, China
E-mail: zhongjin@nju.edu.cn
Z. Tie, Z. Jin
Shenzhen Research Institute of Nanjing University
Shenzhen 518063, China
The ORCID identification number(s) for the author(s) of this article can be found under https://doi.org/10.1002/smll.202102894.

DOI: 10.1002/smll.202102894

of Li^+ will notably impair the energy density and electrode stability. As a result, the exploration of an advanced silicon-based electrode with high ICE has been in the spotlight of research effort to overcome this limitation to further realization of superior electrochemical performance. However, many efforts have been devoted to eliminate the mechanical stress, while few studies have been conducted to focus on the ICE, as shown in **Figure 1**a,b. Nevertheless, over the past several years, we have witnessed steady growth in high-quality works in relation to ICE improvement of SLIBs (Figure 1b), but to our best knowledge, there has so far been no special review that systematically probes and summarizes the research to tackle the problem of the low ICE of SLIBs. From viewpoint of the practical application, the ICE for SLIBs is a very important parameter on the energy density of LIBs when assembling into full batteries, so it is necessary to comprehensively summarize and analyze recent work dedicated to improving the ICE value of Si anodes.

This review is the first work to systematically summarize the representative work from the perspective of ICE values of SLIBs and categorize approaches into several groups based on the influencing factors. The origination of the inferior ICE for SLIBs is analyzed in detail, and solutions and strategies for improving the ICE of SLIBs are thoroughly discussed. As shown in **Figure 2**, we introduce in each part the representative work on ICE engineering in terms of structural regulation, prelithiation, interfacial design, binder design, and electrolyte additive. In addition, some notable works providing new insights for solving the problem are also presented. Finally, conclusions and future approaches for the development of real-world SLIBs are considered.

2. Causes of Low ICE for SLIBs

Alloying-type anode materials usually referring to group IV and V elements, such as Si,[7] Ge,[8] Sn,[9] P,[10] and their oxides,[11] with a mechanism based on alloying reactions that take place between electrodes and lithiums. For SLIBs, the low ICE values primarily stem from Li ion trapping in the host material and SEI film generation during the first lithium-insertion reaction.[12] Hence, from an overall performance viewpoint, for maintaining long-term cycling stability, delicate structure designs including various Si structures fabrication, morphology regulation, as well as composite materials formation, in turn, will sacrifice the ICE.[13] The compromised ICE would exert great influences in assembling full-cells in real-world applications because deteriorative ICE consumes an excess amount of active material used only in the first cycle, leading to a diminished total energy density.[14] For reference, current commercial LIBs with graphite anodes usually possess ICEs higher than 85% at low resistances (≈0.1 C).[14b,15]

On the other hand, the electrolytes of lithium-ion batteries are usually composed of cricoid carbonic esters (e.g., ethylene carbonate (EC) and propylene carbonate (PC)), and linear dimethyl carbonate (DMC), diethyl carbonate (DEC) and ethyl methyl carbonate (EMC). Concurrently, they also contain solvated lithium salts (e.g., $LiPF_6$, $LiClO_4$, $LiBF_6$, or lithium bis(trifluoromethanesulfonyl)imide tetrahydrofuran(LiTFSI)).[16] It is imagined that electrolytes will undergo irreversible decomposition at low potentials (0.8–2.0 V) due to their thermodynamic instability.[17] The decomposition voltage is depend on the species of electrolyte used, added components such as vinylene carbonate (VC) or vinyl fluorocarbonate (VFC), and the scanning speed. As a result, a solid electrolyte interphase (SEI) film with a thickness ranging from several to hundreds of angstroms (Å) will be formed on the electrode.[18] The average thickness of the SEI film can be measured via electrochemical impedance spectroscopy (EIS). The compositions of SEIs are very complex, and some of them are easily dissolved in the electrolyte. When the electrolyte is reduced, some inorganic salts (e.g., Li_2CO_3, LiF, Li_2O) and organics (e.g., $(CH_2OCO_2Li)_2$, polyethylene oxide, and polycarbonate) derived from the decomposition of solvated lithium salts and solvent molecules are formed competitively.[19] In general, inorganic films have a tendency to adhere to electrodes, and organic films deposit on them. In typical cases, an SEI film forms constantly with deep cycling; however, most of the lithium consumption appears in the first cycle. Ideally, the further decomposition of the electrolytes will be impeded by the presence of the SEI film. Hence, the quality and stability of SEI films play a pivotal role in the overall performance and safety of batteries.

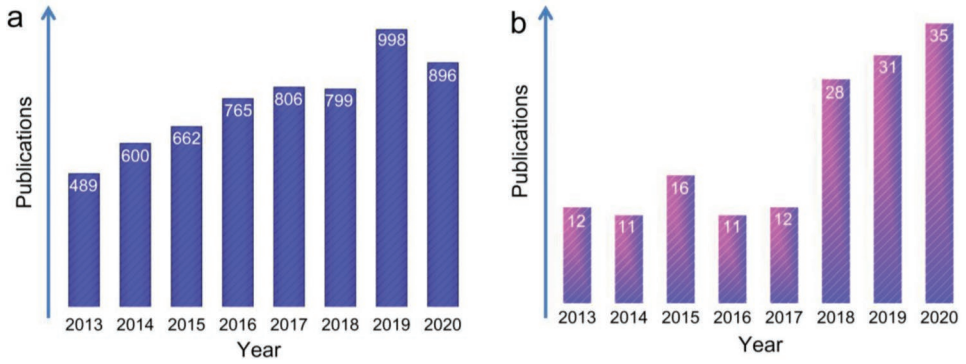

Figure 1. Numbers of publications found by searching key words: a) "silicon lithium-ion battery" and b) "silicon initial Coulombic efficiency" in the Web of Science.

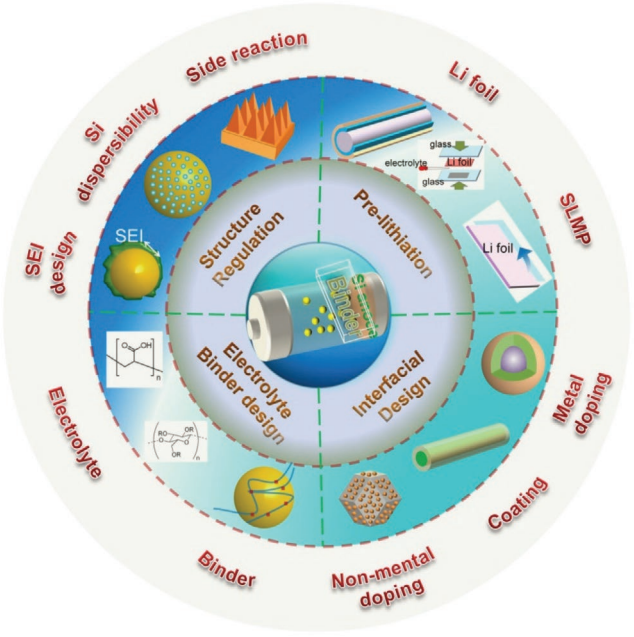

Figure 2. Overview of the proposed strategies for improving ICE of LIBs with Si anodes.

3. Solutions and Strategies for Improving ICE Values of Si Anodes

3.1. Structure Regulation of Electrode Materials

The large volume changes undergone by Si anodes during lithiation/delithiation process exert significant impacts on the Coulombic efficiency and cycling stability.[20] Therefore, alleviating the volume effects by material design, especially reducing the size of the host active material from bulk to nanoscale, is regarded as one of the most efficient solutions.[21] The existing methods for structure regulation can be classified into following three categories, including SEI stability derived from the various structures, well-dispersed Si, and balancing the cycling stability and side reactions. In addition, to obtain a comprehensive understanding of the relationship between various structures of Si and the ICE values, we have conducted extensive surveys and summaries, as presented in **Table 1**.

3.1.1. SEI Stability Derived from the Various Structures

The stability of the SEI film formed during the first discharge process in SLIBs is clearly important. It directly determines the ICE value of SLIBs because the generation of SEI film is closely associated with the irreversible consumption of the electrolyte.[45] Hence, it is of great importance to find ways to restrain the ongoing growth of SEI film to improve the ICE and lifespan of SLIBs. Recently, some productive studies regarding morphological control,[46] electrolyte additives,[47] surface modification,[48] and artificial SEI formation[49] have been carried out. For example, Ryu et al. prepared 3D porous Si plates from natural clay via magnesiothermic reduction. After removing the intermediate magnesium oxides, there were many void spaces left both inside and on the outer surface. The porous Si plate electrode delivered outstanding high ICE values comparable to those of various alloyed anode materials, with the ICE value over 92%.[50] In addition, impressive related approaches, such as the pore modulation (**Figure 3**a) within Si hosts, have been proposed to maintain a high ICE value over 80% for SLIBs. Furthermore, the in situ capability of AFM has been used to directly measure SEI growth on Si and the Si volume expansion ratio as a function of its degree of lithiation, as presented in Figure 3b. It should be emphasized that electrode design from the SEI perspective is a broad concept; in many cases, it is closely connected with design of electrolytes and structures.

3.1.2. Well-Dispersed Si

The inherently low electrical conductivity of elemental Si requirs that actual applications of Si anodes can be realized only by the combination of Si with other conductive substrates.[53] Generally, carbonaceous materials are employed preferentially to combine with Si, owing to their high machinability, superior electrical conductivity and moderate price.[54] However, current research related to carbon modifications usually involves physical mixing or chemical coating. It is difficult to achieve a thoroughly uniform distribution of Si in the carbon matrix, which will lead to poor cycling stability and low Coulomb efficiencies.[55] Hence, it is necessary to construct Si/C composite anodes at the atomic scale to realize high electrochemical performance. One of the feasible strategies to establish sub-nanoscale Si/C nanocomposites is designing materials at the molecular level. As presented in **Figure 4**, based on a facile sol-gel and along with pyrolysis method, a porous silicon-based nanocomposite anode derived from phenylene-bridged mesoporous organosilicas (PBMOs) was fabricated by Zhu et al. PBMOs exhibit organic–inorganic hybrid character at molecular scale, and the formed hybrid anode can retain this unique structure, with carbon layer distributed homogeneously in the Si-O-Si framework at the atomic scale.[56] The novel composite electrode exhibited superior cycling stability and the improved Coulomb efficiency up to 95.4%.

Similar work conducted by Lin et al. showed $AlCl_3$-assisted magnesiothermic reduction of phenyl-rich polyhedral silsesquioxanes (POSS) to afford Si/C composites.[57] The obtained Si/C electrode showed ultrahigh cycling stability (over 1000 cycles) and a relatively high ICE value of 73.2%. Therefore it is believed that atomic dispersed Si in carbon and/or other conductive matrics is beneficial for improving the ICE values of Si anodes to some extent due to relatively uniform SEI film generated. It can be briefly summarized that well-dispersed Si, especially at atomic scale is very beneficial for the uniform growth of SEI fim, thus probablly boost the ICE value for SLIBs to some extent. The great research efforts in atomic dispersions of Si in conductive matrices are also made in recent years.

3.1.3. Balancing the Cycling Stability and Side Reactions

Owing to irreversible interactions occurring between active materials and electrolytes during the first lithiation process,

Table 1. Various structures of Si with different ICEs (Note: EC, DEC, FEC, DMC, EMC, and VC represent ethylene carbonate, diethyl carbonate, fluoroethylene carbonate, dimethyl carbonate, ethyl methyl carbonate, and vinylene carbonate, respectively.

Material	Electrolyte	Charge capacity [mA h g^{-1}]	Discharge capacity [mA h g^{-1}]	ICE [%]	Refs.
Si nano-flakes	EC/DEC with 10 wt% FEC	≈2500	≈2800	89	[22]
SiO/C micro-structure	EC/DMC/EMC	1259	≈1751	72	[23]
Si nanoparticle	EC/DMC/DEC with 5% FEC and 2% VC	≈730	≈800	91	[24]
Si-graphite/C	EC/DEC/EMC	687.7	759.2	91	[25]
Porous SiO_x	EC/DEC/EMC with 5% FEC	≈1786.9	2256.2	79	[26]
Porous silicon	EC/DMC	2180.0	2749.1	79	[27]
Si nanoparticle	EC/DMC	644	739.6	90	[28]
Si/SiO_2@C	PA/FEC/DEC with 1 wt% VC	–	–	74	[29]
$Cu@Cu_xSi/SiO_2$	EC/DEC/DMC with 2 wt% VC and 10 wt% FEC	≈2415	≈2800	86	[30]
SiO_x@C	EC/DEC/DMC with 10 wt% FEC	≈1491	1986	75	[31]
Si micro-structure	EC/DEC with 10 wt% FEC	3073	3553	86	[32]
Si/SiO_x-C	EC/DEC with 3 vol% FEC	2167	2851	76	[33]
Silicon@C nanoparticle	EC/DEC/DMC	735.53	845.33	87	[34]
SiO_x/CNT/C	EC/DMC	1400.5	1878.6	75	[35]
Si/graphite/C	EC/DEC/EMC	448	553	81	[36]
Core-shell Si@C	EC/DC/EMC	≈1157.12	≈1404.27	82	[37]
Si-Sb-ZnO	EC/DMC	845.1	1301.5	65	[38]
Porous Si	EC/MEC with 5 wt% VC	3067	3652	84	[39]
Si/graphite/C	EC/EMC/DMC	909.8	1184.6	77	[40]
Si/graphite/C	EC/DEC/EMC	471.5	601.3	78	[41]
SiO@C	DEC/EC with 30 vol% FEC	1280	2058.6	62	[42]
Si@SiC@C	EC/DEC/DMC	≈2108	≈2382	89	[43]
Si@Cu nanowire	EC/DC/DMC	2854.4	3066.9	93	[44]

some side reactions are inevitably happened. Especially for SiO_x electrodes, the severe irreversible reactions will lead to ultralow ICE values.[58] One important consideration for this issue is how to balance the BET surface areas and volume expansion of Si electrodes.[22,59] As shown in **Figure 5**a, Gu et al. investigated the internal factors that affect the ICE values of silicon/graphite (Si/G) composites and found that the low BET surface area of the Si@C-G electrode delivers an ICE value higher than that of Si-G@C.[60] Similarly, as shown in Figure 5b, Li et al. prepared Si/C composites with different carbon locations by adjusting the heating rate and found that the obtained Si/C-1 sample with BET surface area of 32.4 m^2 g^{-1} showed an ICE (87.5%) significantly higher than that of pristine Si with a high BET surface area of 235.6 m^2 g^{-1} (< 50%).[61] In addition, Cao et al. systematically researched the effect of the particle size of AlSi alloy powder on the morphological structure and electrochemical performance, and the results are presented in Figure 5c.[62] The obtained Si spheres with particle sizes of 30, 15, and 2 µm, showed ICE values of 82%, 76%, and 68%, respectively. Notablly, the surface-engineering strategy was also employed to tackled the issue. For example, Wang et al. deposited a dense Si skin onto porous Si microparticles and further encapsulated it with a conformal graphene cage, which boosted the ICE value of SLIBs.[63] Moreover, it should be indicated that the side reactions can-not be merely ascribed to the BET surface alone, but other parameters, such as the oxidation degree of the surface of Si and the types of coated carbon used, also have remarkable influences on the ICE values.

3.2. Prelithiation

The prelithiation technique is deemed as an indispensable procedure for electrochemical energy storage systems, and can effectively make up for irreversible capacity loss, so as to lifting the Li^+ ions concentration in the electrolyte and raise the working voltage.[64] Currently, the prelithiation methods for anode materials can be mainly divided into three categories: prelithiation by direct contact with metal Li foil, stabilized lithium metal powder (SLMP), and chemical/electrochemical prelithiation. Some benefits and shortcomings coexist. To better study prelithiation methods, we deliberately categorized the prelithiation strategies into three types, as shown in **Table 2**.

3.2.1. Prelithiation by Direct Contact with Li Foil

As presented in **Figure 6**, prelithiation by direct contact with Li metal foil is a technique based on a self-discharging mechanism. Due to the potential difference between metallic Li and the electrode, electrons spontaneously migrate to the anodes, and this is accompanied by the insertion of lithium ions while

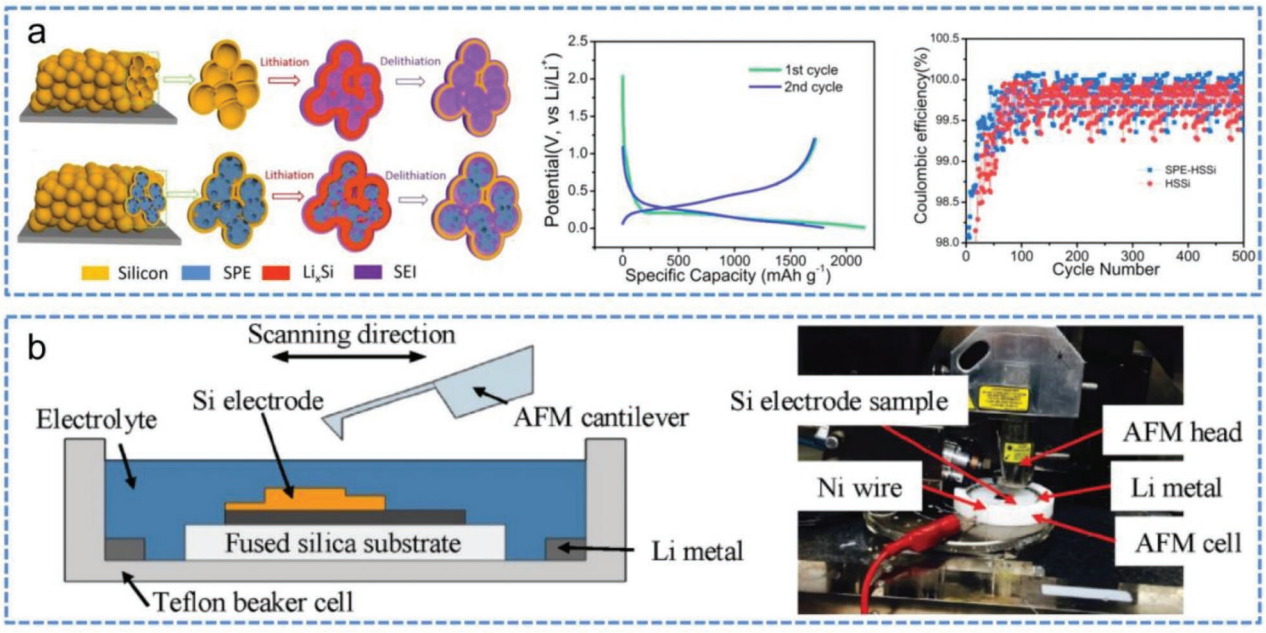

Figure 3. a) Schematic diagram of the lithiation and SEI growth of solid polymer electrolyte-filled hollow structured silicon spheres (SPE-HSSi). Reproduced with permission.[51] Copyright 2017, American Chemical Society; b) Cross-sectional schematic of the AFM "beaker" cell and photograph of the AFM "beaker" cell integrated into an AFM with Ar gas protection. Reproduced with permission.[52] Copyright 2016, Wiley-VCH.

the anode materials are in contact with Li foil in the presence of electrolyte.[91] As shown in **Figure 7**a, after prelithiation, both the initial capacity and the ICE of SLIBs were improved significantly. As such, Liu et al. employed in-situ TEM technique to investigate the dynamic lithiation process of single-crystal silicon with atomic resolution. It is easy to observe the

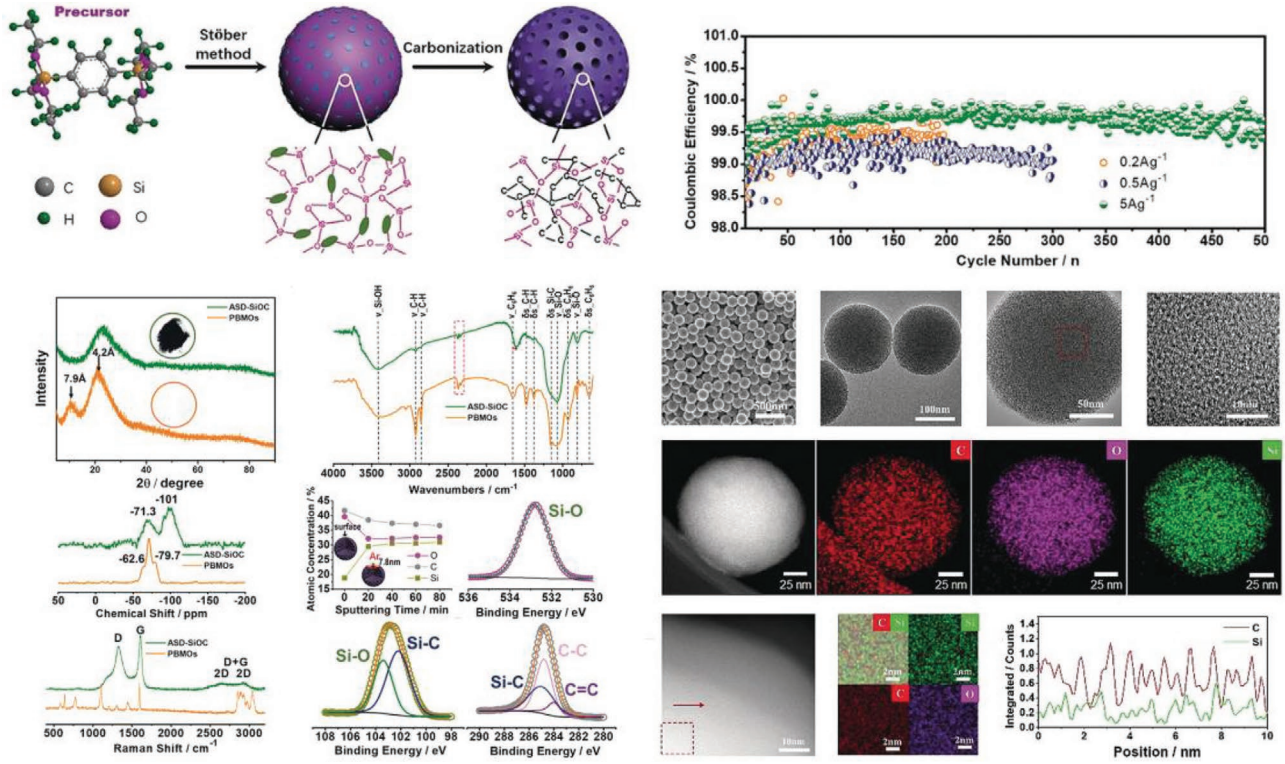

Figure 4. Schematic and characterization of atomic-level SiO_x/C nanocomposites. Reproduced with permission.[56] Copyright 2019, Wiley-VCH.

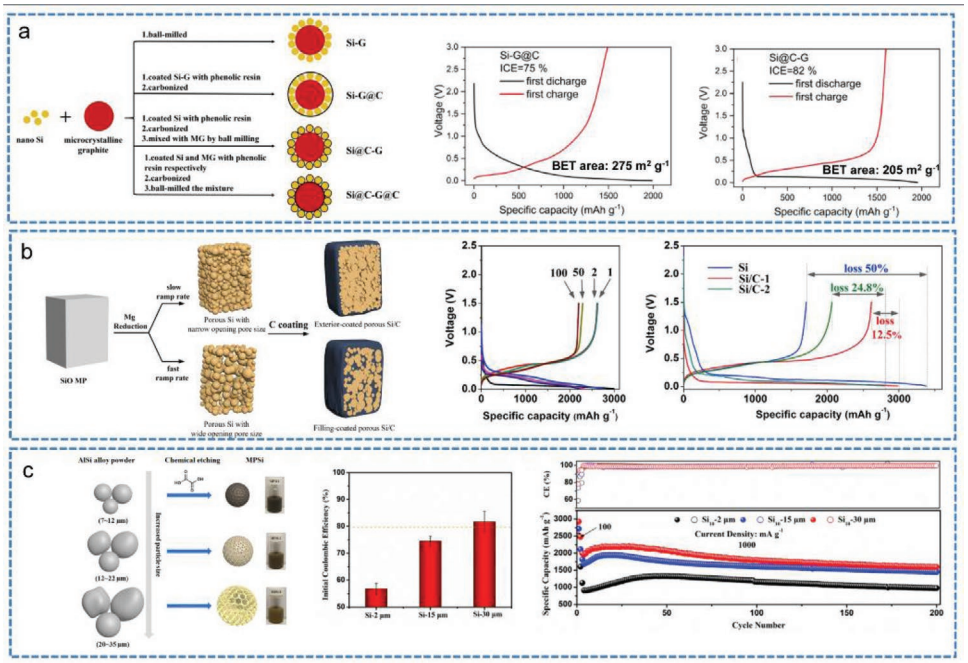

Figure 5. a) Schematic diagram showing the preparation of different Si/C composites and the ICE comparison between Si/C anodes with different BET surface areas. Reproduced with permission.[60] Copyright 2021, Elsevier. b) Fabrication of carbon-coated Si/C microparticles and the corresponding electrochemical performance. Reproduced with permission.[61] Copyright 2017, Elsevier. c) Schematic illustration of the fabrication process of porous Si with different sizes and the corresponding ICE values. Reproduced with permission.[62] Copyright 2019, Elsevier.

sharp interface (≈1 nm thick) between c-Si and amorphous Li_xSi alloy.[92] Although internal short method is convenient and efficient, the degree of prelithiation is extremely hard to control. Thus, an optimized prelithiation strategy based on the direct-contact method is proposed (Figure 7b). In this case, introducing a resistance buffer layer (RBL) between the anode and Li foil could effectively regulate the rate and degree of lithiation. The porous structure and the high electrical conductivity of RBL could boost the transfer of Li^+ and the transport of electrons. In addition, the soft trait of RBL could ensure a close contact and bring out a homogeneous prelithiation. The initial charge-discharge curves of SiO_x electrodes after prelithiation using the RBL method indicated that the ICE value is promoted to 89.2% from 79.4% (without prelithiation).

3.2.2. Stabilized Lithium Metal Powder (SLMP)

In 2005, stabilized lithium metal powder (SLMP), which involved small spherical particles with sizes of approximately 20–30 μm coated by Li_2CO_3 was designed by FMC Lithium Co. (Philadelphia, PA, USA).[94] SLMP is stable in dry air, which makes it effective in compensating for the first cycle Li loss of various anode materials, including Si and graphite. However, preparation of SLMP in the laboratory is difficult. Moreover, due to the large particle size, uniform distribution of SLMP in the anode is still challenging. Furthermore, a pressure activation process is normally required to crack the Li_2CO_3 shell and thus enable contact between active materials and Li metal.[95] As exhibited in **Figure 8**a, Forney et al. utilized SLMP with pressure activation to effectively prelithiate high-capacity Si-carbon nanotube (Si-CNT) anodes, eliminating the 20–40% first cycle irreversible capacity loss.[96] Moreover, based on the traditional SLMP method, Zhao et al. reported Li_xSi-Li_2O core-shell nanoparticles as an excellent prelithiation reagent with a high capacity to compensate for the initial cycle capacity loss.[69] As shown in Figure 8b, these nanoparticles exhibited high capacity under dry air conditions with the protection of a Li_2O passivation shell. Moreover, this approach is considered applicable to various anode materials, including those with complex nanostructures.

As a typical commercial technique, SLMP features some special advantages: 1) the degree of prelithiation can be regulated by controlling the usage of lithium powders; 2) lithium can be uniformly distributed on the surface of the electrode; 3) SLMP is stable in dry air and has high compatibility with the existing battery production process; 4) It can be immediately reacted with anode to form SEI film after contact with the electrolyte; and 5) the lack of residual lithium metal after prelithiation precludes lithium plating.

3.2.3. Chemical/Electrochemical Prelithiation

Chemical/electrochemical prelithiation methods are characterized by convenience, maneuverability and low cost.[97] For instance, Ai and coworkers developed facile and effective approaches to prelithiate hard carbon[98] and silicon anodes[85] by using a spontaneous chemical reaction with lithium naphthalenide (Li-Naph). Due to the moderate reactivity and strong lithiation ability of Li-Naph, hard carbon and silicon anodes

Table 2. Conclusions regarding different prelithiation methods.

Prelithiation Methods	Material	ICE [%]	Ref.
Direct contact with Li foil	SiO_x	89	[65]
	Si-Gr	103	[66]
	Si/graphene oxide nanoribbons	97	[67]
	Si/SiO_2	94	[68]
	Si nanoparticles	>100	[69]
	$LiAlH_4$	88	[70]
	hard carbon/graphene	99	[71]
	SiO_2 particles	>90	[72]
	graphite	100	[73]
Stabilized lithium metal powder (SLMP)	Si nanoparticles-multiwalled carbon nanotubes	98	[74]
	Si@G/C	91	[75]
	micro-sized SiO-based/graphite/carbon	99	[76]
	graphite	≈100	[77]
	Si@C	≈100	[78]
Chemical/electrochemical pre-lithiation	SiO_x	>100	[79]
	SiO	≈91	[80]
	Carbon-coated SiO_x microparticles	90	[81]
	SiO	82	[82]
	Si	93	[83]
	Li_xGe nanoparticles	101	[84]
	silicon nanopowder	96	[85]
	$Si@SiO_x$	89	[86]
	Si nanoparticles	97	[87]
	graphite	93	[88]
	Hard carbon	≈106	[89]

could be prelithiated rapidly and controllably to a desired level by tuning the reaction time, which led to a high ICE of > 93%. However, to date, it is still difficult to dope active Li in high-capacity SLIBs; attempts often merely form SEI film, leading to only partial mitigation of the cycle irreversibility. As presented in **Figure 9**, Jang et al. proposed a molecularly engineered Li-arene complex with a sufficiently low redox potential that enables active Li doping in Si anodes.[99] Fine regulation of the degree of prelithiation and the uniformity of active Li throughout the electrodes were realized by controlling the time and temperature of immersion. It is encouraging that triggering active Li incorporation into SiO_x via Li-arene complex modifications, elevated the initial CE to exceed 100%.

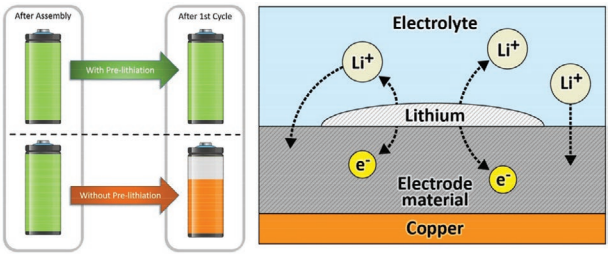

Figure 6. Schematic illustration of the prelithiation process by direct contact to Li metal. Reproduced with permission.[90] Copyright 2018, MDPI, Basel, Switzerland.

The electrochemical prelithiation method, is usually conducted by preassembling a half cell with lithium metal as the counter electrode, as illustrated in **Figure 10**. The required degree of lithiation can be realized by adjusting the number of cycles, the potential, or the cycle time. Thereafter, the prelithiated electrode is separated and reassembled with a fresh anode. Thus far, the electrochemical prelithiation method has been extensively used for the prelithiation of electrodes such as metal oxides,[100] hard/soft carbon,[101] and graphene.[102] Under normal circumstances, two key requirements need to be fulfilled: 1) for finely control of the degree of prelithiation, it is essential to ensure that the prelithiation process is conducted at a low current density, and 2) it is necessary to carry out more cycles to retard side reactions. Certainly, although the electrochemical prelithiation method is controllable and easily operated, the assembly/disassembly of pretreated half-cells will result in expenditures and complicated procedures, which are not beneficial for commercialization.

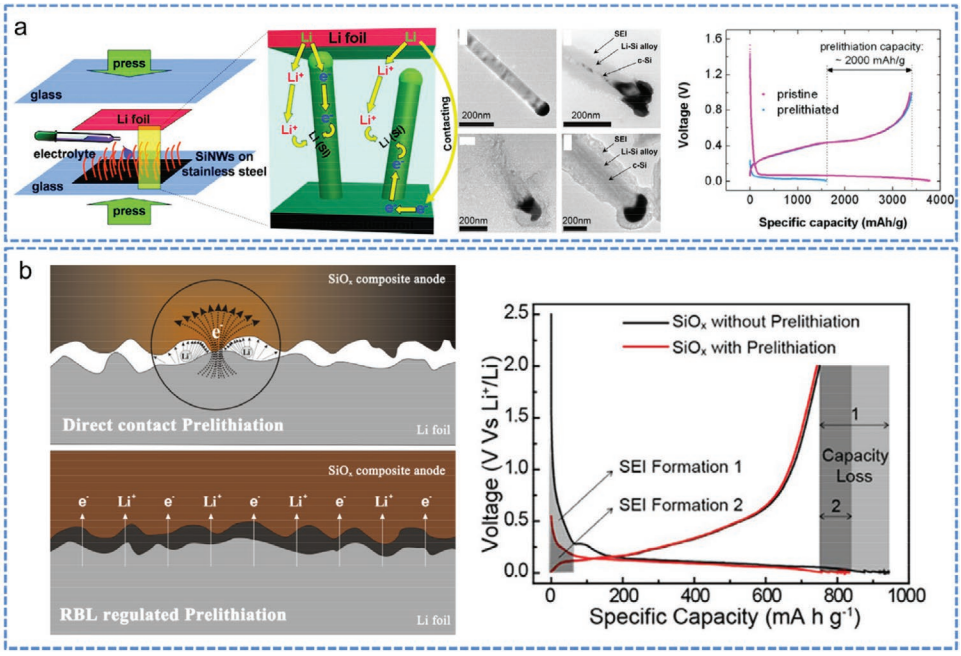

Figure 7. a) Schematic diagrams showing the prelithiation of Si nanowires on stainless steel and the internal electron and Li^+ pathways during prelithiation. Reproduced with permission.[93] Copyright 2011, American Chemical Society. b) Graphical illustration of Li^+ and electron transfer in the direct contact prelithiation process and RBL-regulated prelithiation process, as well as the initial charge and discharge profiles. Reproduced with permission.[65] Copyright 2019, American Chemical Society.

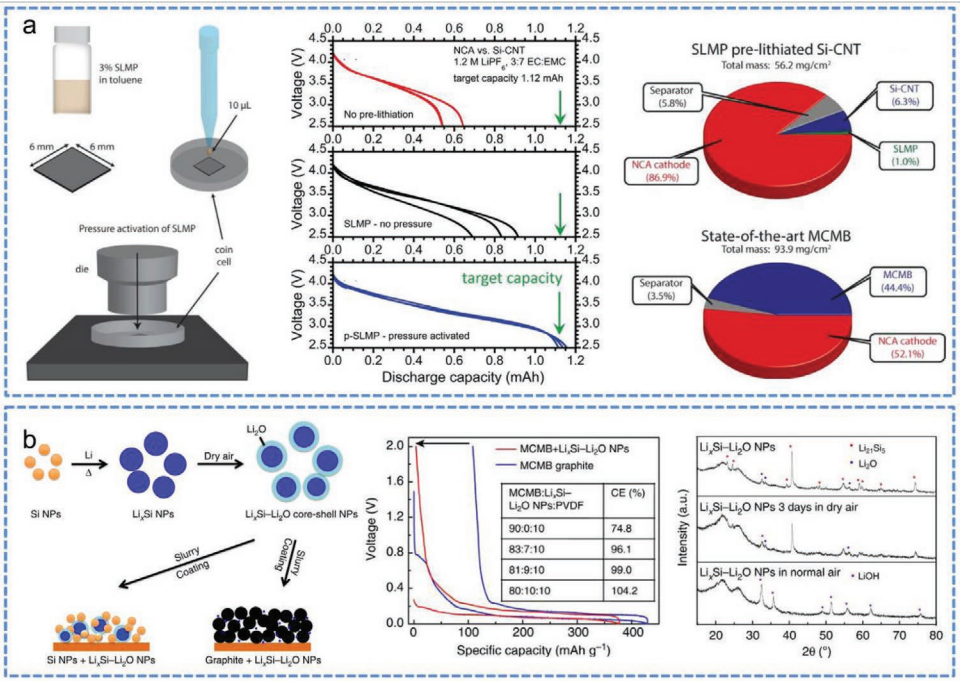

Figure 8. a) Schematic of the SLMP process and the first three voltage-capacity curves of the Si-CNT electrode with and without activated pressure. Reproduced with permission.[96] Copyright 2013, American Chemical Society. b) Schematic diagrams showing Si NPs with melted Li to form Li_xSi NPs. The electrochemical performance and stability of Li_xSi-Li_2O NPs. Reproduced with permission.[69] Copyright 2014, Nature.

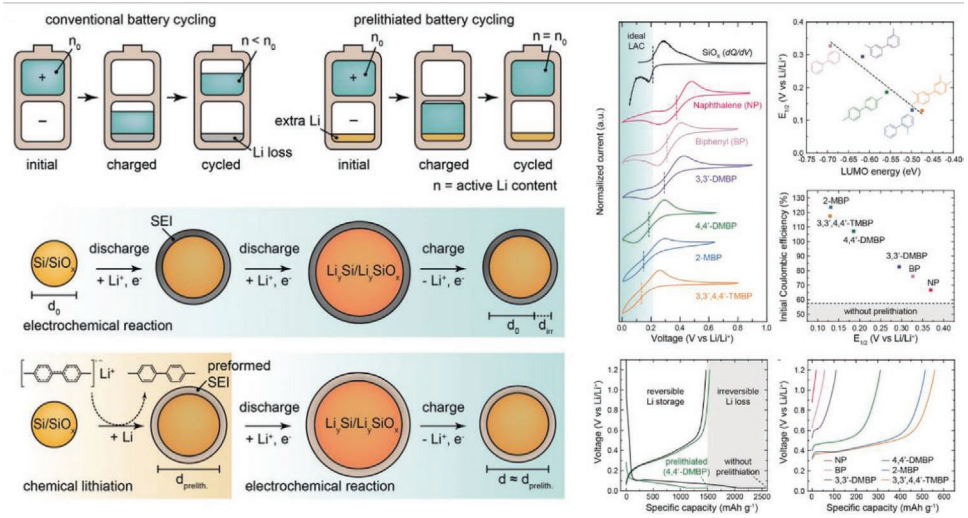

Figure 9. Benefits of prelithiation of high-capacity Si/SiO_x anodes and prelithiation of SiO_x anodes enabled by molecular tailoring of arenes. Reproduced with permission.[99] Copyright 2020, Wiley-VCH.

3.3. Interfacial Design

3.3.1. Coatings

Coating modifications on Si surface represents a high efficient strategy to stabilize the SEI film because the coating layer effectively avoids the direct contact between the electrode and electrolyte. Amongst various coatings, graphitic and/or amorphous carbons are widely used due to their machinability, high conductivity, and low cost. As illustrated in **Figure 11**b, Zhang and coworkers obtained amorphous carbon from the coal tar pitch, when it adheres to the surface of Si, the formed Si@C electrode displayed a high specific capacity of 1314.6 mA h g^{-1} and an ICE of 83.8% because the amorphous carbon could effectively restrain the volume variation of Si; Wang et al. (Figure 11c) designed a cellulose-based topological microscroll by the self-rolling of cellulose nanosheets to fabricate a flexible, binder-free, and free-standing electrode containing an unprecedented 92% Si content.[3e] In this design, carbon-coated Si nanoparticles are not only confined in cellulose carbon rolls, but also anchored on conductive carbon nanotubes. This unique coating design for Si-based anodes enables remarkable electrochemcial performance such as high Si content and improved ICE values (≈85%). Besides carbon substances, some inorganic layers are also employed to modify Si anodes. As shown in Figure 11a, anatase-phase TiO_2 layer was introduced as highly stable interface to embellish Si, this TiO_2 layer gave rise to the decreased resistance to electron and ion diffusion of composite and the improved ICE higher than 81%. The assembled full-battery exhibited an initial area capacity of 2.6 mA h cm^{-2} with an ICE higher than 90%.

3.3.2. Metal/Nonmetal Doping

Carbon coating is considered one of the most effective strategies to boost the electrochemical performance of Si anodes, however, in many cases, amorphous carbon coatings irreversibly react with Li^+ at low potentials, which is unfavorable for the ICE.[105] In addition to carbon modifications, carrier doping is another available pathway to enhancing the conductivities of Si materials.[106] Recently, some metal oxides have been employed to modify anode materials to improve ICE values, and this was attributed to the rapid electron transport and alleviation of side reactions induced by metal components.[107] **Figure 12**a,b show metallic Ag- and Cu- doped Si anodes with significantly improved ICE values. On the other hand, some nonmetal doping strategies were also used to optimize Coulombic efficiency.[108] For example, Chen et al. designed highly crystalline B-doped porous Si (B-doped pSi) nanoplates via the air-oxidation demagnesiation of Mg_2Si from p-type Si wafers. As illustrated in Figure 12c, doping with B greatly decreased the resistance and surface oxidation compared to those of the starting materials.[111] As a result, the obtained B-doped

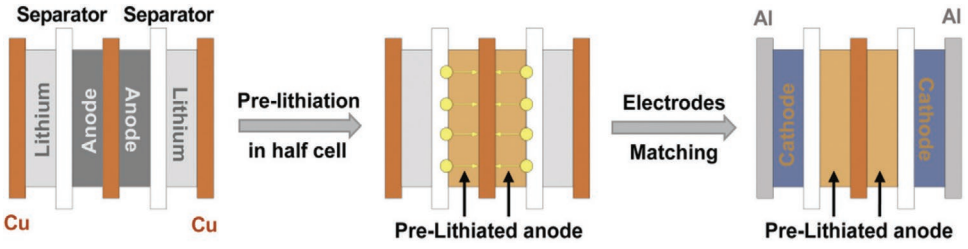

Figure 10. Schematic diagram of the electrochemical prelithiation method. Reproduced with permission.[103] Copyright 2020, Royal Society of Chemistry.

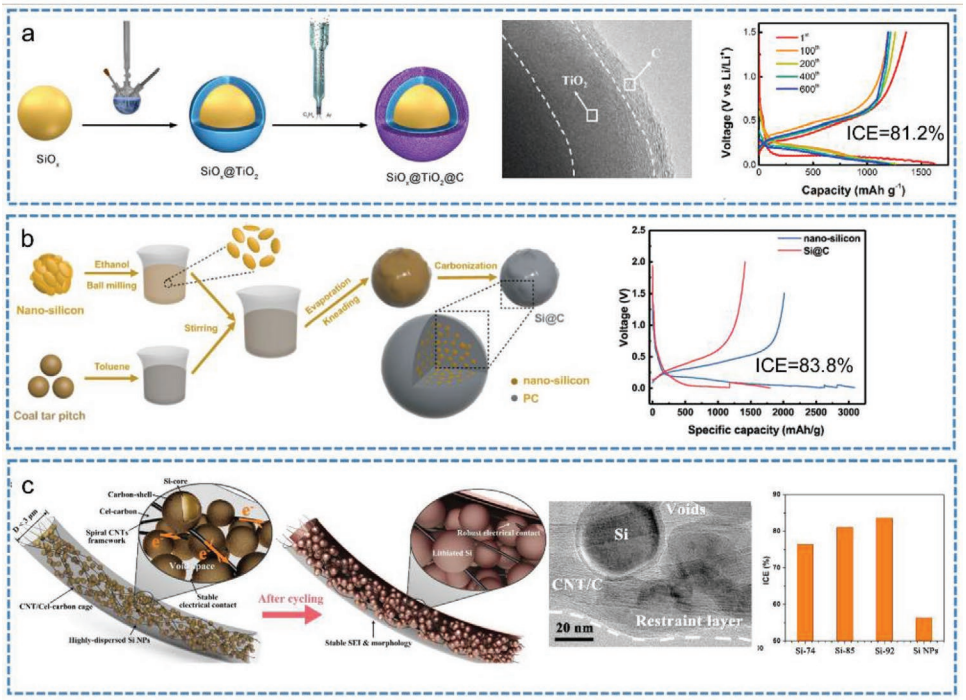

Figure 11. a) Preparation of the SiO_x@TiO_2@C electrode with a high ICE value of 81.2%. Reproduced with permission.[111f] Copyright 2020, Elsevier. b) Schematic illustration of the preparation process of Si@C. Reproduced with permission.[104] Copyright 2020, Royal Society of Chemistry. c) Designed Si@CNT/C microscrolls with high ICEs of over 80%. Reproduced with permission.[3e] Copyright 2020, Royal Society of Chemistry.

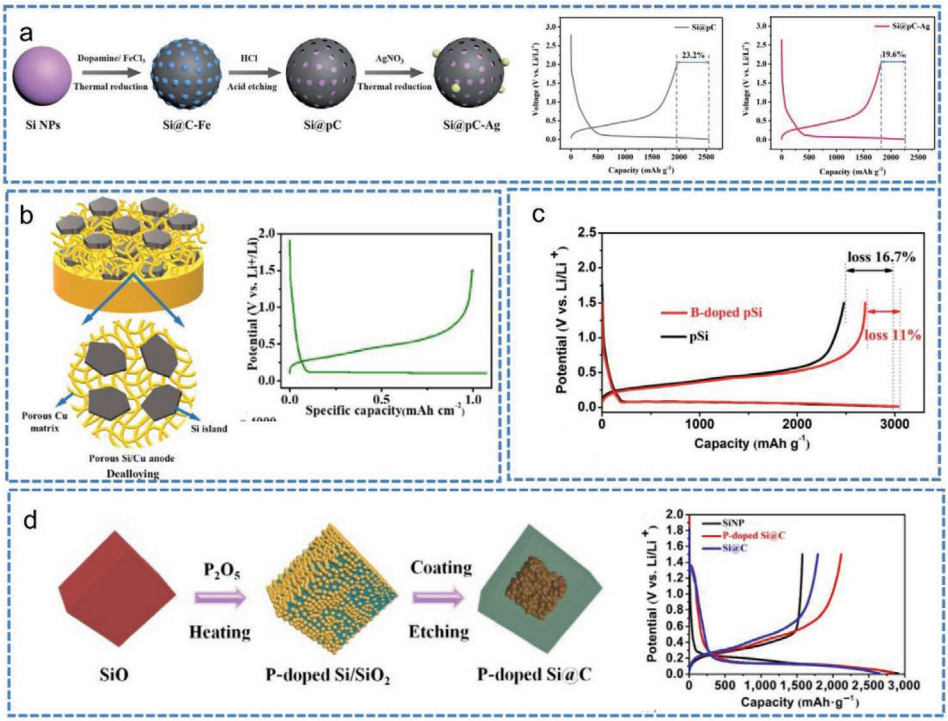

Figure 12. a) Schematic diagram of the preparation of Si@porous C-Ag satellite-like nanoparticles and the comparison of first cycle voltage profiles of Si@porous C and Si@porous C-Ag electrodes. Reproduced with permission.[109] Copyright 2019, Royal Society of Chemistry. b) Schematic of the dealloying process of porous Si/Cu anodes and the corresponding first cycle voltage profile. Reproduced with permission.[110] Copyright 2020, American Chemical Society. c) First discharge/charge curves of B-doped porous Si and porous Si electrodes at 0.4 A g^{-1}. Reproduced with permission.[108b] Copyright 2018, Royal Society of Chemistry. d) Fabrication procedure for the P-doped Si@C material and the comparison of voltage profiles of various Si-based anodes. Reproduced with permission.[111] Copyright 2021, Springer.

Si electrode exhibited a high ICE value of 89%. As another example (Figure 12d), P-doped Si@C electrodes were prepared by Chen and coworkers, delivered a significant increase in Coulombic efficiency from 74.4% to 99.6% after only 6 cycles, high capacity retention of ≈95% over 800 cycles at 4 A g^{-1}, and excellent rate capability (510 mA h g^{-1} at 35 A g^{-1}).

3.4. Binder Design

Conventional polyvinylidene difluoride (PVDF) is one of effective binders that has a spreadwide application in battery domain. However, it is not appropriate for Si anodes owing to the weak van der Waals interactions betweent Si and the copper current collector.[112] Choi et al. discovered that the addition of 5 wt% polyrotaxane into a traditional polyacrylic acid (PAA) binder imparted extraordinary elasticity.[113] As presented in **Figure 13**a, the mode of action of a pulley was proposed to provide a plausible stress-release mechanism. The authors found that polyrotaxane ring components can still move smoothly along the thread component even a partial of them are covalently bonded to the PAA chains, thus acting like moving pulleys to substantially lower the tension exerted on the polymer network. The resulting polymer with highly stretchable and elestic can be realized by incorporation of only 5 wt% polyrotaxane into PAA. which makes even cracked Si particles remain coalesced without collapsion during ever-increasing (de)lithiation. For another example, Li and coworkers proposed a binder-lithiated method for ultrahigh-areal-capacity Si anodes, as illustrated in Figure 13b. Typically, a trifunctional network binder (N-P-LiPN) with hard/soft modulation was constructed with partially lithiated hard polyacrylic acid as a framework and partially lithiated soft Nafion as a buffer via the hydrogen binding effect. This novel binder had both strong adhesion and mechanical properties to accommodate huge volume changes of Si anodes, thus enabling the Si electrode to achieve a highest ICE of 93.18% and an ultrahigh-areal-capacity of 49.59 mA h cm^{-2}.

On the other hand, 3D binder networks were also frequently utilized based on so-called "molecular engineering" to stabilize Si anodes, thus reducing the interfacial side reactions and improving the ICE.[115] **Figure 14**a shows a 3D binder devised with an organic polyvinyl alcohol (PVA) skeleton cross-linked by a functional boric acid (BA). A high ICE of 92.8% with excellent rate performance (≈2920.7 mA h g^{-1} at 10 C) was achieved after optimization of some key parameters. Another study carried out by Zhang and coworkers showed that the employment of a self-healable supramolecular polymer, which was prepared by copolymerization of tert-butyl acrylate and a ureido-pyrimidinone monomer followed by hydrolysis, significantly relieved the side reactions caused by volume changes of silicon hosts. An electrode using this supramolecular polymer as the binder delivered an initial discharge capacity as high as 4194 mA h g^{-1} and a Coulombic efficiency of 86.4%, and reached a high capacity of 2638 mA h g^{-1} after 110 cycles (Figure 14b), elucidating a significant improvement in the electrochemical performance relative to those of Si anodes using conventional binders.

3.5. Electrolyte Additive

Electrolytes are considered the media for Li^+ transport between the anode and cathode in a packed battery. In general, the electrolytes for Si anodic LIBs contain Li salts, organic solvents (mixture of carbonate esters), and some functional additives. A good electrolyte should meet certain requirements: 1) low viscosity and high ion conductivity at the operating temperature; 2) stability over a wide electrochemical window; 3) chemical inertness; and 4) formation of an effective SEI film on the surface of the Si electrode.[118] In order to improve the ICE values of Si-based LIBs, it is of great importance to design effective additives for the electrolyte.[119] One important cause of the low ICE values for Si anodes is the ever-growing SEI film. Therefore, designing functional electrolyte additives that enable stable formation of SEI films is quite beneficial for increasing the ICE values of Si anodes. Currently, some

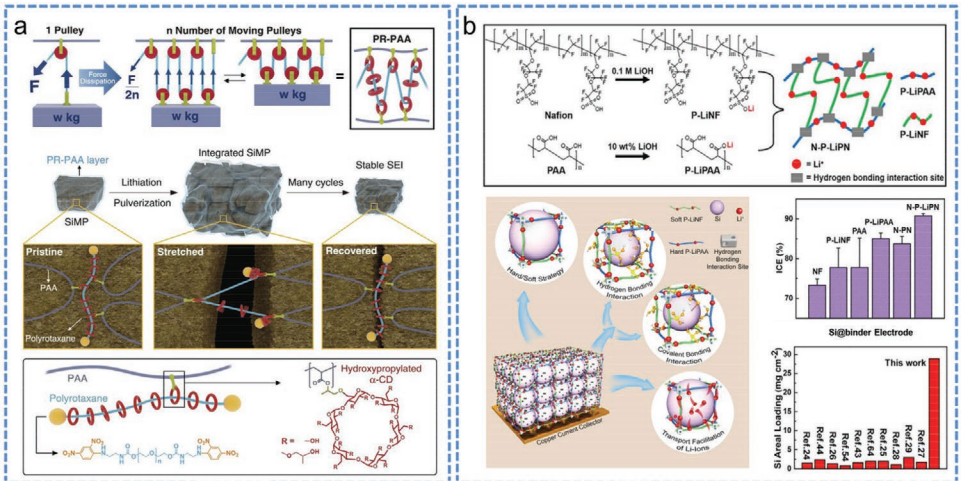

Figure 13. a) The pulley principle used to lower the force in lifting an object and the schematic of the pulverization of the polyacrylic acid-modified Si microparticle electrode. Reproduced with permission.[113] Copyright 2020, Science. b) Preparation scheme of the N-P-LiPN binder and schematic illustration of the functional mechanism of the N-P-LiPN binder in the Si electrode. Reproduced with permission.[114] Copyright 2020, Wiley-VCH.

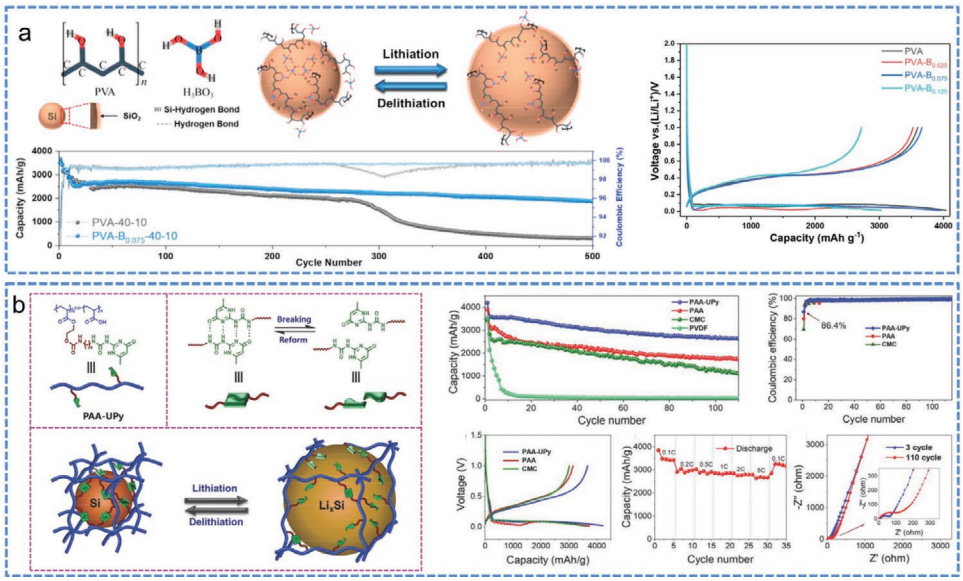

Figure 14. a) Schematic of the cross-linking mechanism for PVA-B complexes, the interaction with —OH on the Si surface, and the electrochemical properties. Reproduced with permission.[116] Copyright 2020, Elsevier. b) Schematic illustration of the PAA-Upy binder for Si anodes and the related electrochemical performance. Reproduced with permission.[117] Copyright 2018, Wiley-VCH.

popular electrolyte additives for Si-based LIBs include fluoroethylene carbonate (FEC) and vinylene carbonate (VC).[120] To elucidate the role of FEC additives in standard carbonate-based electrolytes, Jin et al. combined solution and solid-state NMR techniques to analyze the formed SEI film.[121] As shown in **Figure 15**, a linear oligomeric electrolyte consisting of soluble poly(ethylene oxide) breakdown products was observed after cycling in the presence of 10 vol% FEC additive. The FEC additive in the electrolyte allowed the generation of a stable SEI and suppressed the decomposition of the ethylene carbonate (EC)/dimethyl carbonate (DMC) solvents, thus increasing the Coulombic efficiency.

Apart from FEC and VC, some novel electrolyte additives have also been developed to improve the ICE values of Si-based LIBs. For example, Liu et al. introduced tris(trimethylsiyl)-phosphite (TMSPi) as an electrolyte additive to improve the electrochemical performance of Si/graphite full cells through the formation of protective surface layers at the electrode/electrolyte interface.[122] As shown in **Figure 16**a, the ICE value significantly increased after TMSPi was added. Figure 16b,c illustrated

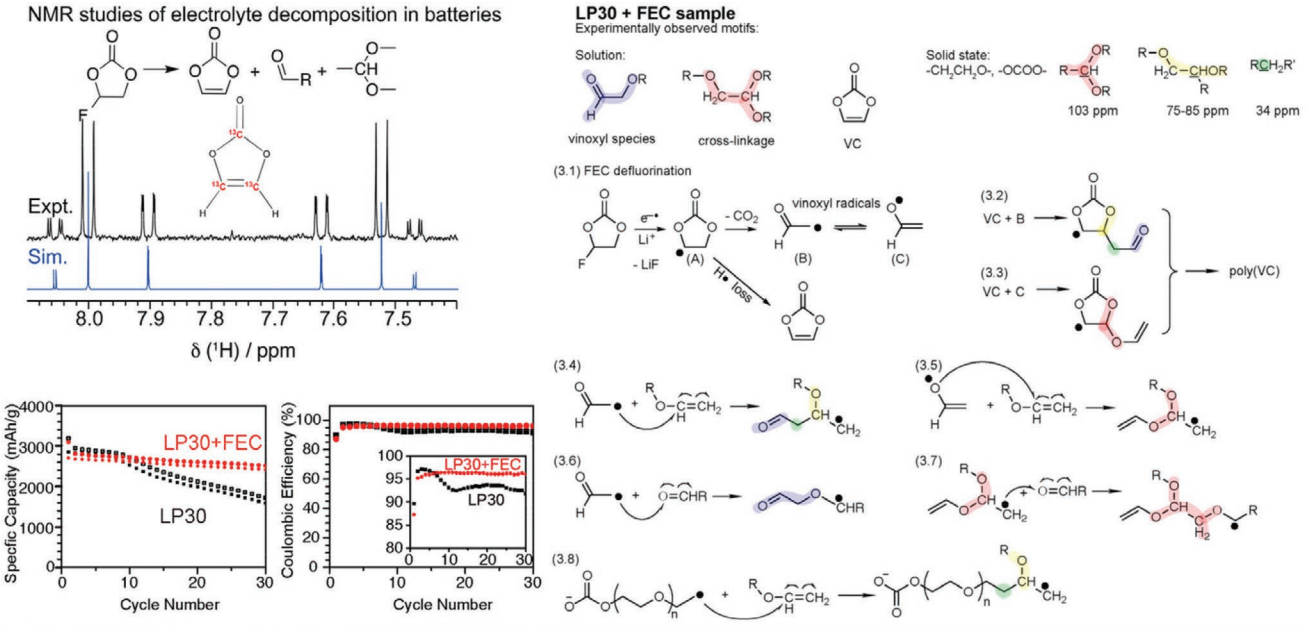

Figure 15. NMR spectra, synthesis of the FEC additive, and comparison of electrochemical performances for LP30 and LP30 + FEC. LP30 represents EC/DMC (1:1 vol%). Reproduced with permission.[121] Copyright 2017, American Chemical Society.

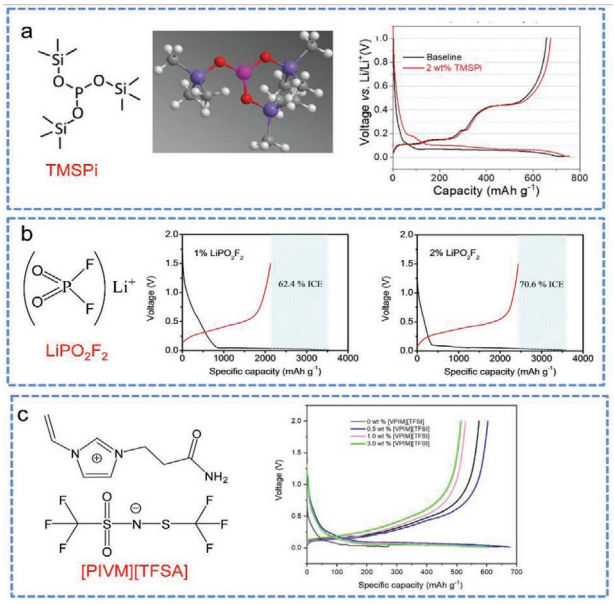

Figure 16. a) 2D and 3D structures of tris-(trimethylsiyl)-phosphite (TMSPi) and the first cycle voltage profile of Si anodes with and without TMSPi added. Reproduced with permission.[122] Copyright 2020, Wiley-VCH. b) Structure of $LiPO_2F_2$ and the ICE comparison with different amounts of $LiPO_2F_2$. Reproduced with permission.[123] Copyright 2020, Wiley-VCH. c) Chemical formula of ionic liquid [PIVM][TFSA] and the first cycle voltage profile observed after adding [PIVM][TFSA] in different proportions. Reproduced with permission.[124] Copyright 2020, Elsevier.

the use of $LiPO_2F_2$ and ionic liquid [PIVM][TFSA] as electrolyte additives, and both effectively increased the ICE values of Si-based anodes. Due to the utmost importance of electrolytes during the formation of SEI films, it is believed that the modification of electrolyte design to boost the electrochemical performance of Si-based anodes in batteries is still an important research area.

3.6. Other New Insights

Recently, some new insights for increasing the ICE of silicon anodes have been developed. For instance, Zhu et al. were inspired by the "isovalent isomorphism" method that is commonly used with solid electrolytes, in which similar but larger ions replace the primary ions to facilitate ion transport.[125] As shown in **Figure 17**, Ge atoms were added to a Si anode using a convenient ball milling method, and they increased Li migration and effectively improved the initial CE of the Si-based anode to over 90% (the highest value reached was 94.1%). Ge dopant atoms expanded the lattice, which greatly reduced the energy barrier for Li diffusion, thereby minimizing Li trapping. In addition, to address the arising new issue of low ICE of Si anodes along with the nanostructuring Si host material to alleviate the volume expansion, a dense silicon layer onto each mesoporous Si microparticle and further encapsulating it with a conformal graphene cage was developed by Cui and coworkers to boost the ICE value of a Si anode.[60] After the surface engineering treatment, both the ICE and later-cycle Coulombic efficiencies were improved due to the minimized side reactions and the reduced electrode/electrolyte contact area.

4. Conclusion and Future Perspectives

Silicon is considered to be one of the most promising anode materials for next- generation state-of-the-art high-energy lithium ion batteries (LIBs), owing to its ultrahigh theoretical capacity, proper working potential and high abundance. However, the inherently large volume expansion, unstable SEI layer and poor conductivity of Si have hindered its further practical application. In the past decade, many research papers and reviews have been published regarding structural designs to alleviate the large volume changes and prolong the lifespans of silicon-based LIBs. However, it is necessary to emphasize that one of the key parameters that affects the performance of Si anode full-cell system is the ICE value. ICE has an important impact on the utilization of the active material and the weight of a practical battery. On the other hand, some important research progress related to the ICE values of Si anodes has been made in recent years. Therefore, it is crucial to conduct a comprehensive survey of the achievements. Unfortunately, to date, there has been no review systematically summarizing related works. Consequently, in this review, we have discussed and summarized recent advances in boosting ICE values of Si anodes by way of structure regulation, prelithiation, interfacial design, electrolyte design and binder design, and through other insights. For each part, further detailed categories were divided, and full discussions were presented. The overall advantages and defects of each approach are illustrated in **Figure 18** along with reported data. In addition, we list some important directions for future research and development:

1) Over the past decade, the deteriorative issue of low ICE values for Si anodes has been partially addressed through various methods. In particular, structural design is believed to be the most effective solution, and it involves the construction of silicon nanostructures (downsizing Si to the nanoscale with various morphologies, dimensions and porous structures) and fabrication of silicon composites (compositing with carbon, metal, metal oxide and conductive polymers). Regulating Si structures by stabilizing the SEI film seems promising for improving ICE value; however, it should be noted that balancing the side reactions and the electrode stability is of great importance because nano-scaled structures of Si are beneficial for the lifespan but are harmful to the ICE value. Especially for SiO_x anodes, the presence of oxide layer on the surface of the Si-based material has been regarded as an effective promoter for enhanced cycle life performance. However, the severe side reactions between the SiO_x electrode and electrolytes will lead to the dramatically decrement of the ICE value. Therefore, it is reasonable to consider both ICE and cycling stability when designing and fabricating Si nanostructures.
2) The design of novel electrolyte additives and binders with both extension strength and flexibility is urgent. Although the SEI film is featured with complexity in the composition, the Coulombic efficiency of Si anodes is highly dependent

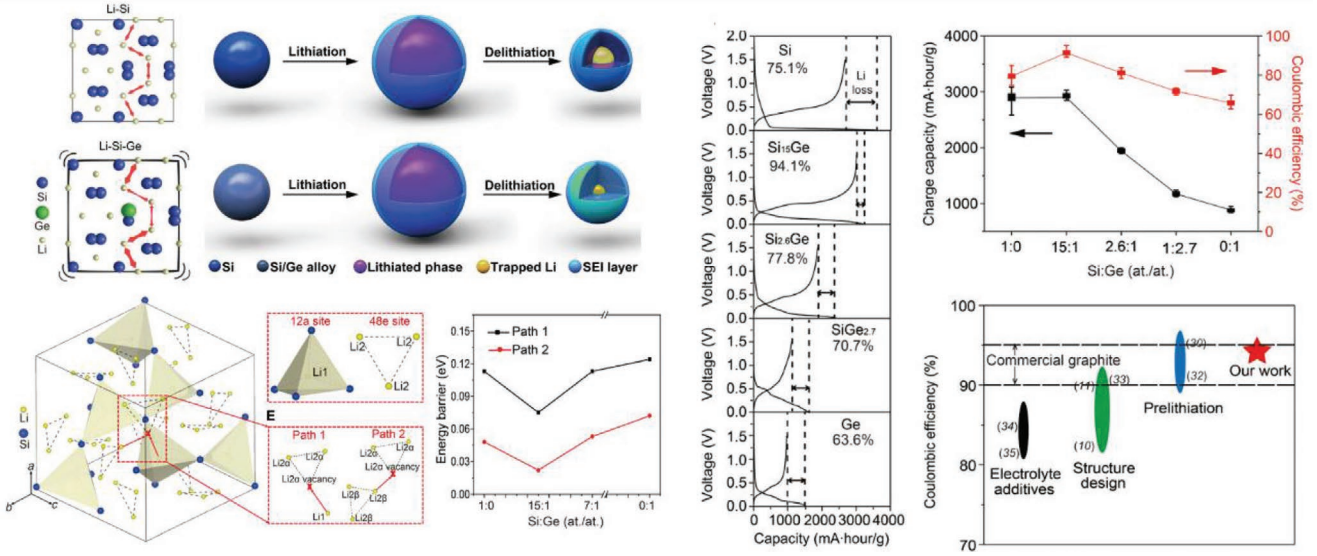

Figure 17. Schematics, calculations, and first cycle voltage profiles of Si anodes with different Ge contents. Reproduced with permission.[125] Copyright 2019, Science.

on electrolyte composition, presence of protective additives, impurity concentration, charge/discharge condition, etc.[126] Electrolyte additives could help to stabilize the generated SEI film; concurrently, the high stability of electrodes could be realized by novel binders. It should be considered that the traditional role of a binder is merely to act as a adhesive network to support active materials and electronically conducting diluents such as carbon black on the current collector. However, with the flourish of high-capacity alloyed electrodes, it is momentous to design polymer binders that serve multifunctionalities (e.g., mechanical robustness, superior adhesion capability, and good dispersion). To this end, it is possible to develop Si anodes with high ICE values from the perspective of novel electrolyte additives and binders.

3) Prelithiation is a necessary and powerful strategy to effectively boost the ICE values of Si anodes. However, it should be indicated that the current prelithiation method usually involves complex procedures and/or high costs. In addition, from the perspective of prelithiation mechanism, the limiting factors for prelithiation kinetics and the Li^+ ion diffusion mechanism need to be better understood with the assistance of theoretical calculations and experiments. Concurrently, after prelithiation process, it is indispensable to pay close attention to the characterization and regulation of the SEI film. On the other hand, in terms of practical applications, it is of great importance to look for appropriate Li sources for prelithiation technologies. Thus, it is meaningful to conduct on-going researches and develop some new methodologies to facilitate the prelithiation process, especially in facile operations and avoid multiple steps. In order to realize the commercialization of chemical prelithiation, it is still challenging to develop more active lithium reagents with sufficiently low redox potentials to compensate the loss of Li ions within various anodes. It should be noticed that the compatibility between the prelithiation reagent and the electrode binder needs further consideration. Additionally, since the electrode after chemical prelithiation is unstable in air, the suitable method to improve the air stability of the prelithiated electrode needs to be developed.
4) Strategies attempt to minimize the oxides on the surface of Si. The inevitable presence of Si oxides will result in severe irreversible side reactions during the first delithiation process, thus leading to significantly reduced ICE values. However, on another side, some investigations have revealed that the presence of partially oxided Si is beneficial for prolonging the lifespan, so it is somewhat controversial. In order to obtain Si anodes with both high ICE and superior cycling stability, new insights from the design and controllable preparation of Si with atomic dispersion in graphitic carbon and/or Si with protective groups on its surface, should be emphasized. Indeed, it is a balanced plan that improves the ICE value and reduces the cycling stability.
5) Advanced techniques are urgently needed to characterize SEIs. Although many techniques have been used to probe the formation of SEIs, such as Fourier transform infrared (FT-IR) spectroscopy, X-ray absorption fine structure (XAFS) spectroscopy, and X-ray photoelectron spectroscopy (XPS), the in-depth mechanisms of the formation, growth, and evolution of actual films are still ambiguous. On the other hand, current in situ cells are incapable of completely mimicking real battery operating conditions, and detailed information related to reaction mechanisms, and electron and ion transport kinetics at the electrode/electrolyte interface is still missing due to the complexity of these processes. Thus, it is highly desirable to develop integrated techniques that can access all information at the same time so that a more complete picture can be developed for rational design of electrode materials.

Last but not least, for practical applications, some important factors other than Coulombic efficiency and cycling stability should be carefully evaluated, including the electrochemical performance with high Si loading amount in full-cells, the safety, and the matched cathodes. In SLIBs, large volume expansion, unstable SEI growth, and electrolyte decomposition

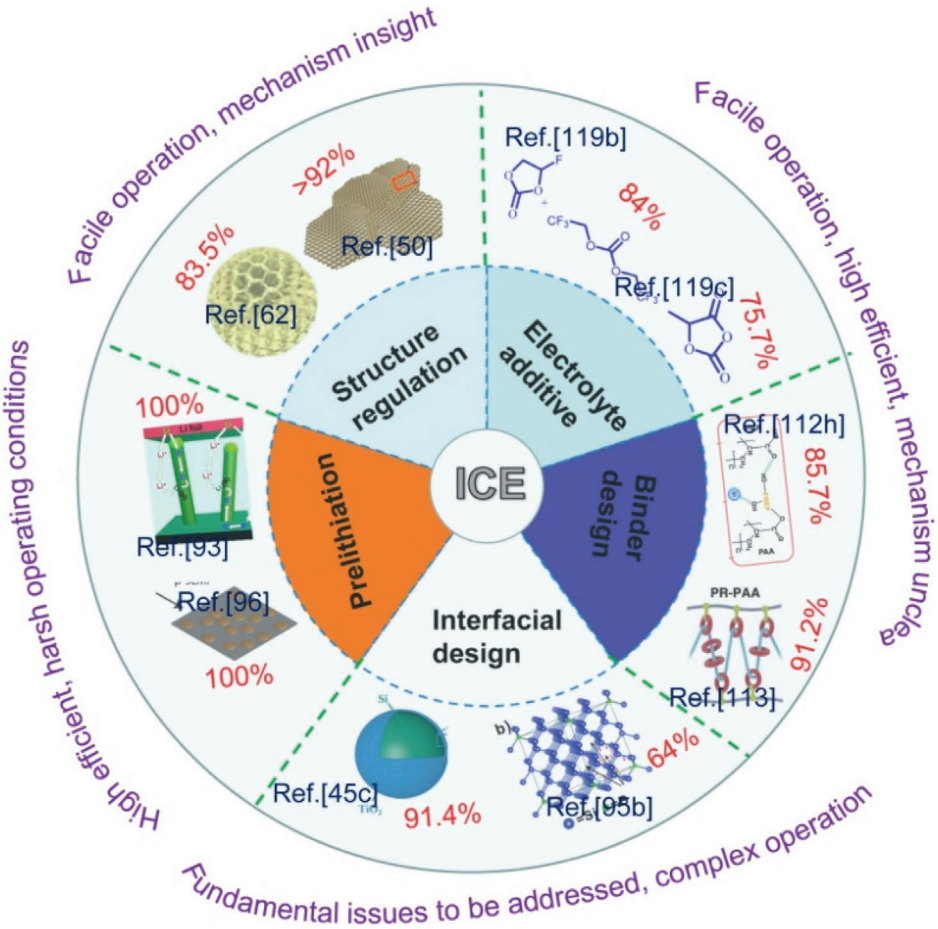

Figure 18. Schematic comparison of different strategies for boosting ICE values of SLIBs. Structure regulation: Reproduced with permission.[50] Copyright 2016, American Chemical Society,[62] Copyright 2019, Elsevier; Electrolyte additive: Reproduced with permission.[119b] Copyright 2016, American Chemical Society,[119c] Copyright 2020, American Chemical Society; Binder design: Reproduced with permission.[112h] Copyright 2020, American Chemical Society,[113] Copyright 2017, Science; Interfaceial design: Reproduced with permission.[45c] Copyright 2021, Elsevier,[95b] Copyright 2019, American Chemical Society; Prelithiation: Reproduced with permission.[93] Copyright 2011, American Chemical Society,[96] Copyright 2013, American Chemical Society.

can give rise to the severe Li dendrite formation which can result in a short circuit and cell explosion. Solid-state batteries using solid electrolytes are a promising candidate to solve this problem and can be fabricated flexibly to drive portable/wearable electronics. Recently, the electrical and ionic conductivity of solid-state batteries are too low for mass production. This immature technology should be pushed quickly toward real-world applications. Certainly, SLIBs have attracted considerable attention as alternatives to traditional graphite LIBs. We believe that with the rapid development and extensive research interest in science and technology in this area, the major stumbling blocks hindering the practical applications of Si anode materials will be overcome successfully in the near future.

Acknowledgements

This work was supported by the National Key Research and Development Program of China (Grant Nos. 2017YFA0208200 and 2016YFB0700600), the Fundamental Research Funds for the Central Universities of China (Grant Nos. 0205-14380219 and 0205-14913212), the Projects of NSFC (Grant Nos. 22022505, 21872069, and 51761135104), the Natural Science Foundation of Jiangsu Province (Grant Nos. BK20181056 and BK20180008), the Shenzhen Fundamental Research Program of Science, Technology and Innovation Commission of Shenzhen Municipality (Grant No. JCYJ20180307155007589), Jiangsu Province Postdoctoral Science Foundation (Grant No. 2020Z258), and Funding for school-level research projects of Yancheng Institute of Technology (Grant No. xjr2019006).

Conflict of Interest

The authors declare no conflict of interest.

Keywords

initial Coulombic efficiency, lithium ion batteries, silicon anodes, structure regulation

Received: May 18, 2021
Revised: July 26, 2021
Published online:

[1] a) M. Chen, X. Ma, B. Chen, R. Arsenault, P. Karlson, N. Simon, Y. Wang, *Joule* **2019**, *11*, 2622; b) G. Harper, R. Sommerville, E. Kendrick, L. Driscoll, P. Slater, R. Stolkin, A. Walton, P. Christensen, O. Heidrich, S. Lambert, A. Abbott, K. Ryder, L. Gaines, P. Anderson, *Nature* **2019**, *575*, 75; c) E. Hosseinzadeh, R. Genieser, D. Worwood, A. Barai, J. Marco, P. Jennings, *J. Power Sources* **2018**, *382*, 77; d) M. Li, J. Lu, Z. Chen, K. Amine, *Adv. Mater.* **2018**, *33*, 1800561; e) F.-Q. Liu, W.-P. Wang, Y.-X. Yin, S.-F. Zhang, J.-L. Shi, L. Wang, X.-D. Zhang, Y. Zheng, J.-J. Zhou, L. Li, Y.-G. Guo, *Sci. Adv.* **2018**, *10*, eaat5383; f) B. Nykvist, M. Nilsson, *Nat. Clim. Change* **2015**, *4*, 329; g) B. K. Peters, K. X. Rodriguez, S. H. Reisberg, S. B. Beil, D. P. Hickey, Y. Kawamata, M. Collins, J. Starr, L. Chen, S. Udyavara, K. Klunder, T. J. Gorey, S. L. Anderson, M. Neurock, S. D. Minteer, P. S. Baran, *Science* **2019**, *6429*, 838; h) X.-G. Yang, T. Liu, C.-Y. Wang, *Nat. Energy* **2021**, *2*, 176.

[2] a) R. Wang, W. Cui, F. Chu, F. Wu, *J. Energy Chem.* **2020**, *48*, 145; b) Y. Sun, G. Zheng, Zhi W. Seh, N. Liu, S. Wang, J. Sun, Hye R. Lee, Y. Cui, *Chem* **2016**, *2*, 287; c) Q. Xu, J.-K. Sun, Y.-X. Yin, Y.-G. Guo, *Adv. Funct. Mater.* **2018**, *8*, 1705235; d) X. Lv, W. Wei, B. Huang, Y. Dai, *J. Mater. Chem. A* **2019**, *5*, 2165.

[3] a) L. Lin, X. Xu, C. Chu, M. K. Majeed, J. Yang, *Angew. Chem., Int. Ed.* **2016**, *45*, 14063; b) T. Yoon, T. Bok, C. Kim, Y. Na, S. Park, K. S. Kim, *ACS Nano* **2017**, *5*, 4808; c) P. Kumar, C. L. Berhaut, D. Zapata Dominguez, E. De Vito, S. Tardif, S. Pouget, S. Lyonnard, P.-H. Jouneau, *Small* **2020**, *11*, 1906812; d) J. Shi, L. Zu, H. Gao, G. Hu, Q. Zhang, *Adv. Funct. Mater.* **2020**, *35*, 2002980; e) H. Wang, J. Fu, C. Wang, J. Wang, A. Yang, C. Li, Q. Sun, Y. Cui, H. Li, *Energy Environ. Sci.* **2020**, *3*, 848; f) S. J. Yeom, C. Lee, S. Kang, T.-U. Wi, C. Lee, S. Chae, J. Cho, D. O. Shin, J. Ryu, H.-W. Lee, *Nano Lett.* **2019**, *12*, 8793.

[4] a) L. Wang, N. Lin, J. Zhou, Y. Zhu, Y. Qian, *Chem. Commun.* **2015**, *12*, 2345; b) X. Li, P. Yan, X. Xiao, J. H. Woo, C. Wang, J. Liu, J.-G. Zhang, *Energy Environ. Sci.* **2017**, *6*, 1427; c) H. Song, H. X. Wang, Z. Lin, X. Jiang, L. Yu, J. Xu, Z. Yu, X. Zhang, Y. Liu, P. He, L. Pan, Y. Shi, H. Zhou, K. Chen, *Adv. Funct. Mater.* **2016**, *4*, 524; d) L. Zeng, R. Liu, L. Han, F. Luo, X. Chen, J. Wang, Q. Qian, Q. Chen, M. Wei, *Chem. - Eur. J.* **2018**, *19*, 4841.

[5] a) T. Kennedy, M. Bezuidenhout, K. Palaniappan, K. Stokes, M. Brandon, K. M. Ryan, *ACS Nano* **2015**, *7*, 7456; b) H. Chen, J. Xu, P.-c. Chen, X. Fang, J. Qiu, Y. Fu, C. Zhou, *ACS Nano* **2011**, *10*, 8383; c) S. Pei, J. Guo, Z. He, L.-a. Huang, T. Lu, J. Gong, H. Shao, J. Wang, *Chem. - Eur. J.* **2020**, *27*, 6006; d) O. Burchak, C. Keller, G. Lapertot, M. Salaün, J. Danet, Y. Chen, N. Bendiab, B. Pépin-Donat, C. Lombard, J. Faure-Vincent, A. Vignon, D. Aradilla, P. Reiss, P. Chenevier, *Nanoscale* **2019**, *46*, 22504; e) K. Stokes, H. Geaney, M. Sheehan, D. Borsa, K. M. Ryan, *Nano Lett.* **2019**, *12*, 8829; f) Y. Zhou, H. Guo, G. Yan, Z. Wang, X. Li, Z. Yang, A. Zheng, J. Wang, *Chem. Commun.* **2018**, *30*, 3755.

[6] a) H. He, D. Sun, Y. Tang, H. Wang, M. Shao, *Energy Storage Mater.* **2019**, *23*, 233; b) X. Li, X. Sun, X. Hu, F. Fan, S. Cai, C. Zheng, G. D. Stucky, *Nano Energy* **2020**, *77*, 105143; c) Y. Yang, X. Qu, X. Zhang, Y. Liu, J. Hu, J. Chen, M. Gao, H. Pan, *Adv. Mater.* **2020**, *22*, 1908285; d) J. Wang, G. Zhang, Z. Liu, H. Li, Y. Liu, Z. Wang, X. Li, K. Shih, L. Mai, *Nano Energy* **2018**, *44*, 272; e) W. Li, H. Li, Z. Lu, L. Gan, L. Ke, T. Zhai, H. Zhou, *Energy Environ. Sci.* **2015**, *12*, 3629.

[7] a) W. Zhou, J. Chen, X. Xu, X. Han, M. Chen, L. Yang, S.-i. Hirano, *ACS Appl. Mater. Interfaces* **2021**, *13*, 15216; b) K. Zeng, T. Li, X. Qin, G. Liang, L. Zhang, Q. Liu, B. Li, F. Kang, *Nano Res.* **2020**, *11*, 2987.

[8] a) N. Hohn, X. Wang, M. A. Giebel, S. Yin, D. Müller, A. E. Hetzenecker, L. Bießmann, L. P. Kreuzer, G. E. Möhl, H. Yu, J. G. C. Veinot, T. F. Fässler, Y.-J. Cheng, P. Müller-Buschbaum, *ACS Appl. Mater. Interfaces* **2020**, *41*, 47002; b) S. Fang, Z. Tong, X. Zhang, *Chem. Eng. J.* **2017**, *322*, 188.

[9] a) X. Wu, C. Qian, H. Wu, L. Xu, L. Bu, Y. Piao, G. Diao, M. Chen, *Chem. Commun.* **2020**, *55*, 7629; b) Y. Li, C. Ou, J. Zhu, Z. Liu, J. Yu, W. Li, H. Zhang, Q. Zhang, Z. Guo, *Nano Lett.* **2020**, *3*, 2034.

[10] a) C. Liu, M. Han, Y. Cao, L. Chen, W. Ren, G. Zhou, A. Chen, J. Sun, *Energy Storage Mater.* **2021**, *37*, 417; b) Y. Zhang, L. Wang, H. Xu, J. Cao, D. Chen, W. Han, *Adv. Funct. Mater.* **2020**, *12*, 1909372.

[11] a) X. He, Y. Hu, R. Chen, Z. Shen, K. Wu, Z. Cheng, P. Pan, *Chem. Eng. J.* **2019**, *360*, 1020; b) T. Kajita, T. Itoh, *Phys. Chem. Chem. Phys.* **2017**, *2*, 1003; c) D. McNulty, H. Geaney, Q. Ramasse, C. O'Dwyer, *Adv. Funct. Mater.* **2020**, *51*, 2005073; d) S. Gao, N. Wang, S. Li, D. Li, Z. Cui, G. Yue, J. Liu, X. Zhao, L. Jiang, Y. Zhao, *Angew. Chem., Int. Ed.* **2020**, *6*, 1465; e) J. Wang, X. Wang, B. Liu, H. Lu, G. Chu, J. Liu, Y.-G. Guo, X. Yu, F. Luo, Y. Ren, L. Chen, H. Li, *Nano Energy* **2020**, *78*, 105101; f) Z. Xiao, C. Yu, X. Lin, X. Chen, C. Zhang, H. Jiang, R. Zhang, F. Wei, *Nano Energy* **2020**, *77*, 105082.

[12] a) Y. He, X. Yu, Y. Wang, H. Li, X. Huang, *Adv. Mater.* **2011**, *42*, 4938; b) F. Yang, X. Song, G. Dong, K.-L. Tsui, *Energy* **2019**, *171*, 1173; c) Y. Zheng, M. Ouyang, L. Lu, J. Li, Z. Zhang, X. Li, *J. Power Sources* **2015**, *289*, 81.

[13] a) Y. Son, N. Kim, T. Lee, Y. Lee, J. Ma, S. Chae, J. Sung, H. Cha, Y. Yoo, J. Cho, *Adv. Mater.* **2020**, *37*, 2003286; b) X. Zhang, D. Wang, X. Qiu, Y. Ma, D. Kong, K. Müllen, X. Li, L. Zhi, *Nat. Commun.* **2020**, *1*, 3826.

[14] a) D. Wang, Z. Zhang, B. Hong, Y. Lai, *Chem. Commun.* **2019**, *72*, 10737; b) A. Raza, J. Y. Jung, C.-H. Lee, B. G. Kim, J.-H. Choi, M.-S. Park, S.-M. Lee, *ACS Appl. Mater. Interfaces* **2021**, *6*, 7161.

[15] F. Zhang, J. Yang, *Emergent Mater.* **2020**, *3*, 369.

[16] a) C. R. Yang, Y. Y. Wang, C. C. Wan, *J. Power Sources* **1998**, *1*, 66; b) D. P. Abraham, M. M. Furczon, S. H. Kang, D. W. Dees, A. N. Jansen, *J. Power Sources* **2008**, *1*, 612; c) L. Sun, J. Xie, Z. Chen, J. Wu, L. Li, *Dalton Trans.* **2018**, *30*, 9989.

[17] F. Ospina-Acevedo, N. Guo, P. B. Balbuena, *J. Mater. Chem. A* **2020**, *33*, 17036.

[18] a) M. Nie, D. Chalasani, D. P. Abraham, Y. Chen, A. Bose, B. L. Lucht, *J. Phys. Chem. C* **2013**, *3*, 1257; b) H. Wu, G. Chan, J. W. Choi, I. Ryu, Y. Yao, M. T. McDowell, S. W. Lee, A. Jackson, Y. Yang, L. Hu, Y. Cui, *Nat. Nanotechnol.* **2012**, *5*, 310.

[19] a) L. E. Camacho-Forero, T. W. Smith, P. B. Balbuena, *J. Phys. Chem. C* **2017**, *1*, 182; b) Melissa L. Meyerson, J. K. Sheavly, A. Dolocan, M. P. Griffin, A. H. Pandit, R. Rodriguez, R. M. Stephens, D. A. Vanden Bout, A. Heller, C. B. Mullins, *J. Mater. Chem. A* **2019**, *24*, 14882.

[20] a) Y. Zhou, Y. Yang, G. Hou, D. Yi, B. Zhou, S. Chen, T. D. Lam, F. Yuan, D. Golberg, X. Wang, *Nano Energy* **2020**, *70*, 104568; b) L. Sun, J. Xie, Z. Jin, *Energy Technol.* **2019**, *11*, 1900962.

[21] a) M. A. Rahman, G. Song, A. I. Bhatt, Y. C. Wong, C. Wen, *Adv. Funct. Mater.* **2016**, *5*, 647; b) Q. Chen, R. Zhu, Q. He, S. Liu, D. Wu, H. Fu, J. Du, J. Zhu, H. He, *Chem. Commun.* **2019**, *18*, 2644; c) Y. Zhang, R. Zhang, S. Chen, H. Gao, M. Li, X. Song, H. L. Xin, Z. Chen, *Adv. Funct. Mater.* **2020**, *50*, 2005956; d) L. Sun, F. Wang, T. Su, H. Du, *ACS Appl. Mater. Interfaces* **2017**, *46*, 40386.

[22] X. Zhou, Y. Ren, J. Yang, J. Ding, J. Zhang, T. Hu, J. Tang, *Chem. Commun.* **2018**, *86*, 12214.

[23] Z.-L. Wu, S.-B. Ji, L.-K. Liu, T. Xie, L. Tan, H. Tang, R.-G. Sun, *Rare Met.* **2021**, *40*, 1110.

[24] Q. Xu, J.-Y. Li, Y.-X. Yin, Y.-M. Kong, Y.-G. Guo, L.-J. Wan, *Chem. Asian J.* **2016**, *8*, 1205.

[25] C. Xiao, P. He, J. Ren, M. Yue, Y. Huang, X. He, *RSC Adv.* **2018**, *48*, 27580.

[26] H. Zhang, K. Liu, Y. Liu, Z. Lang, W. He, L. Ma, J. Man, G. Jia, J. Cui, J. Sun, *J. Power Sources* **2020**, *447*, 227400.

[27] Y. Huang, J. Luo, J. Peng, M. Shi, X. Li, X. Wang, B. Chang, *J. Energy Storage* **2020**, *27*, 101075.
[28] Y. Lv, F. Lin, W. Liu, X. Lei, H. Qin, Z. Zhang, L. Wang, *J. Mater. Sci.: Mater. Electron.* **2020**, *14*, 11238.
[29] W. Wu, M. Wang, J. Wang, C. Wang, Y. Deng, *ACS Appl. Energy Mater.* **2020**, *4*, 3884.
[30] W.-F. Ren, J.-T. Li, S.-J. Zhang, A.-L. Lin, Y.-H. Chen, Z.-G. Gao, Y. Zhou, L. Deng, L. Huang, S.-G. Sun, *J. Energy Chem.* **2020**, *48*, 160.
[31] Z. Xiao, C. Yu, X. Lin, X. Chen, C. Zhang, F. Wei, *Carbon* **2019**, *149*, 462.
[32] J. Yang, Y. Nie, H. Zhou, J. Tang, J. Zhang, X. Zhou, *J. Electroanal. Chem.* **2017**, *799*, 424.
[33] C. Hoeltgen, J.-E. Lee, B.-Y. Jang, *Electrochim. Acta* **2016**, *222*, 535.
[34] X. Zhu, X. Jiang, X. Yao, Y. Leng, X. Xu, A. Peng, L. Wang, Q. Xue, *ACS Appl. Mater. Interfaces* **2019**, *49*, 45726.
[35] Y. Liang, X. Xiong, Z. Xu, Q. Xia, L. Wan, R. Liu, G. Chen, S.-L. Chou, *Small* **2020**, *26*, 2000030.
[36] H. Chen, Z. Wang, X. Hou, L. Fu, S. Wang, X. Hu, H. Qin, Y. Wu, Q. Ru, X. Liu, S. Hu, *Electrochim. Acta* **2017**, *249*, 113.
[37] H. Chen, X. Hou, L. Qu, H. Qin, Q. Ru, Y. Huang, S. Hu, K.-h. Lam, *J. Mater. Sci.: Mater. Electron.* **2017**, *1*, 250.
[38] Y. Li, L. Huang, P. Zhang, X. Ren, L. Deng, *Nanoscale Res. Lett.* **2015**, *1*, 414.
[39] J. Zhang, C. Zhang, S. Wu, J. Zheng, Y. Zuo, C. Xue, C. Li, B. Cheng, *Electrochim. Acta* **2016**, *208*, 174.
[40] R. Zhou, H. Guo, Y. Yang, Z. Wang, X. Li, Y. Zhou, *Powder Technol.* **2016**, *295*, 296.
[41] A. Wang, F. Liu, Z. Wang, X. Liu, *RSC Adv.* **2016**, *107*, 104995.
[42] S. Fang, N. Li, T. Zheng, Y. Fu, X. Song, T. Zhang, S. Li, B. Wang, X. Zhang, G. Liu, *Polymers* **2018**, *6*, 610.
[43] C. Yu, X. Chen, Z. Xiao, C. Lei, C. Zhang, X. Lin, B. Shen, R. Zhang, F. Wei, *Nano Lett.* **2019**, *8*, 5124.
[44] H. Zhang, S. Liu, X. Yu, S. Chen, *J. Alloys Compd.* **2020**, *822*, 153664.
[45] a) Y. Gao, R. Yi, Y. C. Li, J. Song, S. Chen, Q. Huang, T. E. Mallouk, D. Wang, *J. Am. Chem. Soc.* **2017**, *48*, 17359; b) A. Wang, S. Kadam, H. Li, S. Shi, Y. Qi, *npj Comput. Mater.* **2018**, *1*, 15; c) Y. Yan, Y. He, X. Zhao, W. Zhao, Z. Ma, X. Yang, *Nano Energy* **2021**, *84*, 105935.
[46] G. Huang, J. Han, Z. Lu, D. Wei, H. Kashani, K. Watanabe, M. Chen, *ACS Nano* **2020**, *4*, 4374.
[47] J. Ming, Z. Cao, Y. Wu, W. Wahyudi, W. Wang, X. Guo, L. Cavallo, J.-Y. Hwang, A. Shamim, L.-J. Li, Y.-K. Sun, H. N. Alshareef, *ACS Energy Lett.* **2019**, *11*, 2613.
[48] C. Li, T. Shi, D. Li, H. Yoshitake, H. Wang, *RSC Adv.* **2016**, *41*, 34715.
[49] Q. Ai, D. Li, J. Guo, G. Hou, Q. Sun, Q. Sun, X. Xu, W. Zhai, L. Zhang, J. Feng, P. Si, J. Lou, L. Ci, *Adv. Mater. Interfaces* **2019**, *21*, 1901187.
[50] J. Ryu, D. Hong, M. Shin, S. Park, *ACS Nano* **2016**, *11*, 10589.
[51] T. Ma, X. Yu, X. Cheng, H. Li, W. Zhu, X. Qiu, *ACS Appl. Mater. Interfaces* **2017**, *9*, 13247.
[52] I. Yoon, D. P. Abraham, B. L. Lucht, A. F. Bower, P. R. Guduru, *Adv. Energy Mater.* **2016**, *12*, 1600099.
[53] a) M. Jeong, S. Ahn, T. Yokoshima, H. Nara, T. Momma, T. Osaka, *Nano Energy* **2016**, *28*, 51; b) K. Adpakpang, J.-e. Park, S. M. Oh, S.-J. Kim, S.-J. Hwang, *Electrochim. Acta* **2014**, *136*, 483.
[54] a) Y. Lin, Y. Chen, Y. Zhang, J. Jiang, Y. He, Y. Lei, N. Du, D. Yang, *Chem. Commun.* **2018**, *68*, 9466; b) L. Sun, T. Su, L. Xu, H.-B. Du, *Phys. Chem. Chem. Phys.* **2016**, *3*, 1521.
[55] M.-S. Wang, L.-Z. Fan, M. Huang, J. Li, X. Qu, *J. Power Sources* **2012**, *219*, 29.
[56] G. Zhu, F. Zhang, X. Li, W. Luo, L. Li, H. Zhang, L. Wang, Y. Wang, W. Jiang, H. K. J. A. C. I. E. Liu, *Angew. Chem., Int. Ed.* **2019**, *58*, 6669.
[57] X. Lin, A. Li, D. Li, H. Song, X. Chen, *ACS Appl. Mater. Interfaces* **2020**, *12*, 15202.
[58] H. Zhang, R. Hu, Y. Liu, X. Cheng, J. Liu, Z. Lu, M. Zeng, L. Yang, J. Liu, M. Zhu, *Energy Storage Mater.* **2018**, *13*, 257.
[59] J. Shi, X. Jiang, J. Sun, B. Ban, J. Li, J. Chen, *J. Colloid Interface Sci.* **2021**, *588*, 737.
[60] Z. Gu, W. Li, Y. Miao, Y. Chen, X. Xia, G. Chen, H. Liu, *Electrochim. Acta* **2021**, *366*, 137424.
[61] B. Li, Z. Xiao, J. Zai, M. Chen, H. Wang, X. Liu, G. Li, X. Qian, *Mater. Today Energy* **2017**, *5*, 299.
[62] W. Cao, K. Han, M. Chen, H. Ye, S. Sang, *Electrochim. Acta* **2019**, *320*, 134613.
[63] J. Wang, L. Liao, H. R. Lee, F. Shi, W. Huang, J. Zhao, A. Pei, J. Tang, X. Zheng, W. Chen, Y. Cui, *Nano Energy* **2019**, *61*, 404.
[64] a) F. Wang, B. Wang, J. Li, B. Wang, Y. Zhou, D. Wang, H. Liu, S. Dou, *ACS Nano* **2021**, *2*, 2197; b) X. Liu, Y. Tan, W. Wang, C. Li, Z. W. Seh, L. Wang, Y. Sun, *Nano Lett.* **2020**, *6*, 4558; c) Y. Zhu, W. Hu, J. Zhou, W. Cai, Y. Lu, J. Liang, X. Li, S. Zhu, Q. Fu, Y. Qian, *ACS Appl. Mater. Interfaces* **2019**, *20*, 18305.
[65] Q. Meng, G. Li, J. Yue, Q. Xu, Y.-X. Yin, Y.-G. Guo, *ACS Appl. Mater. Interfaces* **2019**, *35*, 32062.
[66] K. H. Kim, J. Shon, H. Jeong, H. Park, S. J. Lim, J. S. Heo, *J. Power Sources* **2020**, *459*, 228066.
[67] C. Yao, X. Li, Y. Deng, Y. Li, P. Yang, S. Zhang, J. Yuan, R. Wang, *Carbon* **2020**, *168*, 392.
[68] H. Wu, L. Zheng, J. Zhan, N. Du, W. Liu, J. Ma, L. Su, L. Wang, *J. Power Sources* **2020**, *449*, 227513.
[69] J. Zhao, Z. Lu, N. Liu, H.-W. Lee, M. T. McDowell, Y. Cui, *Nat. Commun.* **2014**, *1*, 5088.
[70] Y. Pang, X. Wang, X. Shi, F. Xu, L. Sun, J. Yang, S. Zheng, *Adv. Energy Mater.* **2020**, *12*, 1902795.
[71] X. Zhang, C. Fan, S. Han, *J. Mater. Sci.* **2017**, *17*, 10418.
[72] Y. Han, X. Liu, Z. Lu, *Appl. Sci.* **2018**, *8*, 1245.
[73] Z. Cao, P. Xu, H. Zhai, S. Du, J. Mandal, M. Dontigny, K. Zaghib, Y. Yang, *Nano Lett.* **2016**, *11*, 7235.
[74] K. Yao, R. Liang, J. P. Zheng, *J. Electrochem. Energy Convers. Storage* **2016**, *1*, 011004.
[75] M. Bai, L. Yang, Q. Jia, X. Tang, Y. Liu, H. Wang, M. Zhang, R. Guo, Y. Ma, *ACS Appl. Mater. Interfaces* **2020**, *42*, 47490.
[76] Q. Pan, P. Zuo, T. Mu, C. Du, X. Cheng, Y. Ma, Y. Gao, G. Yin, *J. Power Sources* **2017**, *347*, 170.
[77] Z. Wang, Y. Fu, Z. Zhang, S. Yuan, K. Amine, V. Battaglia, G. Liu, *J. Power Sources* **2014**, *260*, 57.
[78] M. Marinaro, M. Weinberger, M. Wohlfahrt-Mehrens, *Electrochim. Acta* **2016**, *206*, 99.
[79] G. Zhu, J. Xu, W. Zhao, F. Huang, *ACS Appl. Mater. Interfaces* **2016**, *46*, 31716.
[80] X. Zhang, H. Qu, W. Ji, D. Zheng, T. Ding, D. Qiu, D. Qu, *J. Power Sources* **2020**, *478*, 229067.
[81] M.-Y. Yan, G. Li, J. Zhang, Y.-F. Tian, Y.-X. Yin, C.-J. Zhang, K.-C. Jiang, Q. Xu, H.-L. Li, Y.-G. Guo, *ACS Appl. Mater. Interfaces* **2020**, *24*, 27202.
[82] J. H. Yom, S. W. Hwang, S. M. Cho, W. Y. Yoon, *J. Power Sources* **2016**, *311*, 159.
[83] Y. Domi, H. Usui, D. Iwanari, H. Sakaguchi, *J. Electrochem. Soc.* **2017**, *7*, A1651.
[84] J. Zhao, J. Sun, A. Pei, G. Zhou, K. Yan, Y. Liu, D. Lin, Y. Cui, *Energy Storage Mater.* **2018**, *10*, 275.
[85] Y. Shen, J. Zhang, Y. Pu, H. Wang, B. Wang, J. Qian, Y. Cao, F. Zhong, X. Ai, H. Yang, *ACS Energy Lett.* **2019**, *7*, 1717.
[86] W. M. Dose, J. Blauwkamp, M. J. Piernas-Muñoz, I. Bloom, X. Rui, R. F. Klie, P. Senguttuvan, C. S. Johnson, *ACS Appl. Energy Mater.* **2019**, *7*, 5019.
[87] J. Zhao, Z. Lu, H. Wang, W. Liu, H.-W. Lee, K. Yan, D. Zhuo, D. Lin, N. Liu, Y. Cui, *J. Am. Chem. Soc.* **2015**, *26*, 8372.

[88] J. Jang, H. Ki, Y. Kang, M. Son, F. M. Auxilia, H. Seo, I.-H. Kim, K.-H. Kim, K.-H. Park, Y. Kim, W. B. Kim, M.-H. Ham, I. S. Kim, *Energy Fuels* **2020**, *10*, 13048.
[89] X. Zhang, H. Qu, W. Ji, D. Zheng, T. Ding, C. Abegglen, D. Qiu, D. Qu, *ACS Appl. Mater. Interfaces* **2020**, *10*, 11589.
[90] F. Holtstiege, O. Bärmann, R. Nölle, M. Winter, T. Placke, *Batteries* **2018**, *1*, 4.
[91] P. Bärmann, M. Diehl, L. Göbel, M. Ruttert, S. Nowak, M. Winter, T. Placke, *J. Power Sources* **2020**, *464*, 228224.
[92] X. H. Liu, J. W. Wang, S. Huang, F. Fan, X. Huang, Y. Liu, S. Krylyuk, J. Yoo, S. A. Dayeh, A. V. Davydov, S. X. Mao, S. T. Picraux, S. Zhang, J. Li, T. Zhu, J. Y. Huang, *Nat. Nanotechnol.* **2012**, *11*, 749.
[93] N. Liu, L. Hu, M. T. McDowell, A. Jackson, Y. Cui, *ACS Nano* **2011**, *8*, 6487.
[94] C. R. Jarvis, M. J. Lain, Y. Gao, M. Yakovleva, *J. Power Sources* **2005**, *1*, 331.
[95] a) B. Huang, T. Huang, L. Wan, A. Yu, *ACS Sustainable Chem. Eng.* **2021**, *2*, 648; b) Y. Ren, X. Zhou, J. Tang, J. Ding, S. Chen, J. Zhang, T. Hu, X. Yang, X. Wang, J. Yang, *Inorg. Chem.* **2019**, *58*, 4592.
[96] M. W. Forney, M. J. Ganter, J. W. Staub, R. D. Ridgley, B. J. Landi, *Nano Lett.* **2013**, *9*, 4158.
[97] G. Wang, F. Li, D. Liu, D. Zheng, Y. Luo, D. Qu, T. Ding, D. Qu, *ACS Appl. Mater. Interfaces* **2019**, *9*, 8699.
[98] Y. Shen, J. Qian, H. Yang, F. Zhong, X. Ai, *Small* **2020**, *7*, 1907602.
[99] J. Jang, I. Kang, J. Choi, H. Jeong, K.-W. Yi, J. Hong, M. Lee, *Angew. Chem., Int. Ed.* **2020**, *34*, 14473.
[100] a) P. Sennu, V. Aravindan, Y.-S. Lee, *Chem. Eng. J.* **2017**, *324*, 26; b) X. Yu, J. Deng, C. Zhan, R. Lv, Z.-H. Huang, F. Kang, *Electrochim. Acta* **2017**, *228*, 76.
[101] a) O. Bolufawi, A. Shellikeri, J. P. Zheng, *Batteries* **2019**, *4*, 74; b) X. Sun, X. Zhang, W. Liu, K. Wang, C. Li, Z. Li, Y. Ma, *Electrochim. Acta* **2017**, *235*, 158; c) X. Sun, X. Zhang, K. Wang, N. Xu, Y. Ma, *J. Solid State Electrochem.* **2015**, *8*, 2501.
[102] a) Y. Ma, H. Chang, M. Zhang, Y. Chen, *Adv. Mater.* **2015**, *36*, 5296; b) Y. Sun, J. Tang, F. Qin, J. Yuan, K. Zhang, J. Li, D.-M. Zhu, L.-C. Qin, *J. Mater. Chem. A* **2017**, *26*, 13601; c) J. J. Ren, L. W. Su, X. Qin, M. Yang, J. P. Wei, Z. Zhou, P. W. Shen, *J. Power Sources* **2014**, *264*, 108.
[103] L. Jin, C. Shen, A. Shellikeri, Q. Wu, J. Zheng, P. Andrei, J.-G. Zhang, J. P. Zheng, *Energy Environ. Sci.* **2020**, *8*, 2341.
[104] W. Zhang, S. Fang, N. Wang, J. Zhang, B. Shi, Z. Yu, J. Yang, *Inorg. Chem. Front.* **2020**, *13*, 2487.
[105] a) S. Guo, X. Hu, Y. Hou, Z. Wen, *ACS Appl. Mater. Interfaces* **2017**, *48*, 42084; b) Y. Ma, H. Tang, Y. Zhang, Z. Li, X. Zhang, Z. Tang, *J. Alloys Compd.* **2017**, *704*, 599.
[106] a) M. Ge, J. Rong, X. Fang, C. Zhou, *Nano Lett.* **2012**, *5*, 2318; b) X. Chen, K. Gerasopoulos, J. Guo, A. Brown, R. Ghodssi, J. N. Culver, C. Wang, *Electrochim. Acta* **2011**, *14*, 5210.
[107] a) W. Luo, D. Shen, R. Zhang, B. Zhang, Y. Wang, S. X. Dou, H. K. Liu, J. Yang, *Adv. Funct. Mater.* **2016**, *43*, 7800; b) B. D. Polat, O. Keles, K. Amine, *Nano Lett.* **2015**, *10*, 6702; c) S. Yoo, J.-I. Lee, S. Ko, S. Park, *Nano Energy* **2013**, *6*, 1471.
[108] a) Y. Ren, X. Zhou, J. Tang, J. Ding, S. Chen, J. Zhang, T. Hu, X.-S. Yang, X. Wang, J. Yang, *Inorg. Chem.* **2019**, *7*, 1592; b) M. Chen, B. Li, X. Liu, L. Zhou, L. Yao, J. Zai, X. Qian, X. Yu, *J. Mater. Chem. A* **2018**, *7*, 3022; c) M. Han, J. Li, J. Yu, *Energy Technol.* **2020**, *7*, 2000351; d) Y. Zeng, Y. Huang, N. Liu, X. Wang, Y. Zhang, Y. Guo, H.-H. Wu, H. Chen, X. Tang, Q. Zhang, *J. Energy Chem.* **2021**, *54*, 727.
[109] F. Zhang, G. Zhu, K. Wang, X. Qian, Y. Zhao, W. Luo, J. Yang, *J. Mater. Chem. A* **2019**, *29*, 17426.
[110] L. Cao, T. Huang, Q. Zhang, M. Cui, J. Xu, R. Xiao, *ACS Appl. Mater. Interfaces* **2020**, *51*, 57071.
[111] M. Chen, Q. Zhou, J. Zai, A. Iqbal, T. Tsega, B. Dong, X. Liu, Y. Zhang, C. Yan, L. Zhao, A. Nazakat, S. E , C. Low, X. Qian, *Nano Res.* **2021**, *4*, 1004.
[112] a) I. Kovalenko, B. Zdyrko, A. Magasinski, B. Hertzberg, Z. Milicev, R. Burtovyy, I. Luzinov, G. Yushin, *Science* **2011**, *6052*, 75; b) B. Koo, H. Kim, Y. Cho, K. T. Lee, N.-S. Choi, J. Cho, *Angew. Chem., Int. Ed.* **2012**, *35*, 8762; c) T.-w. Kwon, Y. K. Jeong, I. Lee, T.-S. Kim, J. W. Choi, A. Coskun, *Adv. Mater.* **2014**, *47*, 7979; d) H. Zhao, Y. Wei, R. Qiao, C. Zhu, Z. Zheng, M. Ling, Z. Jia, Y. Bai, Y. Fu, J. Lei, X. Song, V. S. Battaglia, W. Yang, P. B. Messersmith, G. Liu, *Nano Lett.* **2015**, *12*, 7927; e) C. Wang, H. Wu, Z. Chen, M. T. McDowell, Y. Cui, Z. Bao, *Nat. Chem.* **2013**, *12*, 1042; f) Y. K. Jeong, T.-w. Kwon, I. Lee, T.-S. Kim, A. Coskun, J. W. Choi, *Energy Environ. Sci.* **2015**, *4*, 1224; g) N. Salem, M. Lavrisa, Y. Abu-Lebdeh, *Energy Technol.* **2016**, *2*, 331; h) H. Liu, T. Chen, Z. Xu, Z. Liu, J. Yang, J. Chen, *ACS Appl. Mater. Interfaces* **2020**, *12*, 54842.
[113] S. Choi, T.-w. Kwon, A. Coskun, J. W. Choi, *Science* **2017**, *357*, 279.
[114] Z. Li, Y. Zhang, T. Liu, X. Gao, S. Li, M. Ling, C. Liang, J. Zheng, Z. Lin, *Adv. Energy Mater.* **2020**, *20*, 1903110.
[115] a) Y. Wang, H. Xu, X. Chen, H. Jin, J. Wang, *Energy Storage Mater.* **2021**, *38*, 121; b) Y. Cai, Y. Li, B. Jin, A. Ali, M. Ling, D. Cheng, J. Lu, Y. Hou, Q. He, X. Zhan, F. Chen, Q. Zhang, *ACS Appl. Mater. Interfaces* **2019**, *50*, 46800; c) W.-F. Ren, J.-B. Le, J.-T. Li, Y.-Y. Hu, S.-Y. Pan, L. Deng, Y. Zhou, L. Huang, S.-G. Sun, *ACS Appl. Mater. Interfaces* **2021**, *1*, 639; d) P. Li, G. Chen, Y. Lin, F. Chen, L. Chen, N. Zhang, Y. Cao, R. Ma, X. Liu, *Macromol. Chem. Phys.* **2020**, *2*, 1900414.
[116] Z. Cao, X. Zheng, W. Huang, Y. Wang, Q. Qu, H. Zheng, *J. Power Sources* **2020**, *463*, 228208
[117] G. Zhang, Y. Yang, Y. Chen, J. Huang, T. Zhang, H. Zeng, C. Wang, G. Liu, Y. Deng, *Small* **2018**, *29*, 1801189.
[118] J. Zheng, M. H. Engelhard, D. Mei, S. Jiao, B. J. Polzin, J.-G. Zhang, W. Xu, *Nat. Energy* **2017**, *3*, 17012.
[119] a) K. Wang, L. Xing, H. Zhi, Y. Cai, Z. Yan, D. Cai, H. Zhou, W. Li, *Electrochim. Acta* **2018**, *262*, 226; b) H. Jo, J. Kim, D. Nguyen, K. Kang, D. Jeon, A. Yang, S. Song, *J. Phys. Chem. C* **2016**, *120*, 22466; c) R. Nölle, J. Schmiegel, M. Winter, T. Placke, *Chem. Mater.* **2020**, *1*, 173.
[120] a) L. Chen, K. Wang, X. Xie, J. Xie, *J. Power Sources* **2007**, *2*, 538; b) Q. Li, X. Liu, X. Han, Y. Xiang, G. Zhong, J. Wang, B. Zheng, J. Zhou, Y. Yang, *ACS Appl. Mater. Interfaces* **2019**, *15*, 14066.
[121] Y. Jin, N.-J. H. Kneusels, P. C. M. M. Magusin, G. Kim, E. Castillo-Martínez, L. E. Marbella, R. N. Kerber, D. J. Howe, S. Paul, T. Liu, C. P. Grey, *J. Am. Chem. Soc.* **2017**, *42*, 14992.
[122] H. Liu, A. J. Naylor, A. S. Menon, W. R. Brant, K. Edström, R. Younesi, *Adv. Mater. Interfaces* **2020**, *15*, 2000277.
[123] C. Li, W. Zhu, B. Lao, X. Huang, H. Yin, Z. Yang, H. Wang, D. Chen, Y. Xu, *ChemElectroChem* **2020**, *18*, 37438.
[124] Y. Cai, T. Xu, N. von Solms, H. Zhang, K. Thomsen, *Electrochim. Acta* **2020**, *340*, 135990.
[125] B. Zhu, G. Liu, G. Lv, Y. Mu, Y. Zhao, Y. Wang, X. Li, P. Yao, Y. Deng, Y. Cui, J. Zhu, *Sci. Adv.* **2019**, *11*, eaax0651.
[126] S. Zhang, M. He, C.-C. Su, Z. Zhang, *Curr. Opin. Chem. Eng.* **2016**, *13*, 24.

Lin Sun received his M.S. degree in Chemical Engineering, from the School of Petrochemical Engineering, Changzhou University (2010–2013). He obtained the Ph.D. degree in Chemistry from Nanjing University (2014–2017). His research interests are focused on preparing multifunctional inorganic materials of importance in energy and environmental science by using new synthetic methods and strategies under the guidance of modern computational chemistry.

Yanxiu Liu received her B.S. degree from the College of Food Science and Light Industry at Nanjing Tech University in 2020. She is currently a master's candidate under the supervision of Dr. Lin Sun in the School of Chemistry and Chemical Engineering at Yancheng Institute of Technology. Her research is mainly focused on the synthesis of functional inorganic materials for Si anodes and Li-S batteries.

Zhong Jin received his B.S. degree and Ph.D. degree in Chemistry from Peking University in 2003 and 2008, respectively. Then, he pursued postdoctoral studies at Rice University (2008–2010) and MIT (2010–2014). Since 2014, he has been appointed as a professor at Nanjing University, China. His research is focusing on the nanostructural design, interfacial engineering and mechanism studies of redox-active or redox-promoting electrode materials for clean energy conversion and storage device applications, such as secondary batteries, fuel cells, solar cells and photocatalytic/electrocatalytic systems.